# Injury Biomechanics of the Human Eye During Blunt and Blast Loading

**Vanessa Dawn Alphonse**

Thesis submitted to the faculty of the
Virginia Polytechnic Institute and State University
in partial fulfillment of the requirements for the degree of

Master of Science
in
Biomedical Engineering

Stefan M. Duma, Chair
Joel D. Stitzel
Andrew R. Kemper
Pamela J. Vandevord

26 March 2012
Blacksburg, Virginia

Keywords: eye, injury, risk, blunt, blast, trauma

# Injury Biomechanics of the Human Eye during Blunt and Blast Loading

Vanessa D. Alphonse

## Abstract

The research presented in this thesis investigates eye injuries caused by blunt impacts and blast overpressure. This research represents part of an ongoing investigation to accurately quantify and predict eye injuries and injury mechanisms for various loading schemes. It has been shown that blunt trauma can cause severe eye injuries but it remains undecided whether blast overpressure alone can cause eye injury. Presented herein are four experimental studies that quantify eye injuries and implement a technique for predicting injury risk. Isolated porcine or human eyes were subjected to various loading conditions consisting of blunt projectiles, water streams, remote control helicopter blades, and blast overpressure. All eyes were prepared in a similar manner that required the insertion of a miniature pressure sensor into the globe through the optic nerve. This sensor measured intraocular pressure throughout each event. Using previously published injury risk curves, this intraocular pressure data was used to predict the injury risk for four eye injuries: hyphema, lens damage, retinal damage, and globe rupture. Injuries sustained were quantified upon direct inspection of the globe following testing. No serious eye injuries were observed for any of the tests and all tests resulted in low predicted injury risks consistent with the lack of observed injury. The research presented in this thesis provides a robust low injury level dataset for eye injuries. This data could be useful for designing and validating computational models and anthropomorphic test device eyes, and serves as a basis for future work with more dangerous projectiles and higher pressure levels.

## Acknowledgements

I would like to thank my family for their support of my continued education. Additionally, I would like to acknowledge the co-authors of the chapters presented herein: Stephanie M. Beeman, Jill A. Bisplinghoff, Stefan M. Duma, Andrew R. Kemper, Craig McNally, Steven Rowson, Danielle M. Senge, and Brock T. Strom III.

# Table of Contents

## List of Figures

## List of Tables

# Chapter 1:
# Introduction

## Context

The studies presented in this thesis investigate eye injuries associated with the misuse of various consumer products. Previous research has shown that blunt impacts to the eye can cause serious eye injuries. Blast injuries to the eye have not been well documented and the specific injury mechanism remains unclear. One critical question investigated here is whether blast overpressure from fireworks can cause ocular injury or if injuries are caused solely by projected material (blunt loading). The studies presented in this thesis were conducted sequentially and findings build on information gained in the previous studies. As such, the research presented in this thesis represents a portion of the investigation to determine the specific injury mechanism of blunt and blast trauma, and leaves available many avenues for future related work.

## Eye Injuries

The eye injuries of interest in this study, listed from least damaging to most damaging, are corneal abrasion, hyphema, lens damage, retinal damage, and globe rupture. Corneal abrasions are caused by scraping or shearing the outermost layer of epithelial cells from the cornea. These minor injuries cause mild irritation but often resolve on their own without complication. The extent of corneal abrasion can be easily visualized under a blue light with the aid of fluorescein dye which stains the abraded surfaces. Hyphema is caused by trauma to the eye and is easily detected by the presence of blood pooling in the front of the eye. These injuries can resolve on their own depending on the amount of blood that pools and the ability of the body to resorb this blood. Medical intervention is required when there is sufficient pooling of blood to raise the intraocular pressure in the eye. Lens damage and dislocation often decreases the visual acuity of a patient, leading to the dependence of glasses or contact lenses for vision. Retinal damage may result in the loss of sight and retinal detachment requires prompt medical treatment to mitigate permanent damage. Globe ruptures result in tearing the membranes of the eye to expose the inner portions of the eye. Globe rupture is a severe eye injury that can result in removal of the eye.

# Chapter 2:
# Evaluating the Risk of Eye Injuries: Intraocular Pressure During High Speed Projectile Impacts


## Abstract

**Purpose:** To evaluate the risk of eye injuries by determining intraocular pressure during high speed projectile impacts.

**Methods:** A pneumatic cannon was used to impact eyes with a variety of projectiles at multiple velocities. Intraocular pressure was measured with a small pressure sensor inserted through the optic nerve. A total of 36 tests were performed on 12 porcine eyes with a range of velocities between 6.2 m/s and 66.5 m/s. Projectiles selected for the test series included a 6.35 mm diameter metal ball, a 9.25 mm diameter aluminum rod, and an 11.16 mm diameter aluminum rod. Experiments were designed with velocities in the range of projectile consumer products such as toy guns.

**Results:** A range of intraocular pressures ranged between 2041 mmHg to 26418 mmHg (39 psi - 511 psi). Four of the 36 impacts resulted in globe rupture.

**Conclusions:** Intraocular pressures dramatically above normal physiological pressure were observed for high speed projectile impacts. These pressure data provide critical insight to chronic ocular injuries and long term complications such as glaucoma and cataracts.



**Keywords:** Ocular trauma, Intraocular pressure, Glaucoma, Cataracts


## Introduction

Each year approximately 2 million people in the United States suffer eye injuries that require treatment [1]. The most common sources of eye injuries include automobile accidents [2-12], sports related impacts [13, 14], consumer products [15], and military combat [16]. These events result in nearly 500,000 cases of lost eyesight in the United States each year [17]. In addition to affecting quality of life, the injuries are expensive to treat given the estimated annual cost associated with adult vision problems in the United States of $51.4 billion [18, 19].

In order to predict and possibly prevent eye injuries for various impact scenarios, previous research investigated ocular injuries from projectile impacts with known projectile characteristics [13, 20, 21]. Duma et al. (2005) studied diameter, mass, velocity, kinetic energy, and normalized energy to determine the best ocular injury predictor. A logistic regression analysis concluded

that normalized energy was the most significant predictor of injury type and tissue lesion. Kennedy (2010) reported values for human 50% injury risk of corneal abrasion, lens dislocation, hyphema, retinal damage, and globe rupture [22]. This presented useful for predicting eye injuries given known projectile characteristics. However, there are many cases of blunt trauma where these variables are unknown and the measurement of intraocular pressure is useful.

Previous studies used intraocular pressure to determine the rupture pressure for the human eye [23-26]. Intraocular pressure was dynamically induced within the eye and measured by a small pressure sensor inserted through the optic nerve. High rate pressurization resulted in a mean rupture pressure of 7275 ± 2175 mmHg (141 ± 42.1 psi) [23]. Other studies show lower values for quasi-static loading [27-29]. This study provides pressure results for the most severe eye injuries, but additional data is needed to represent the less severe injuries that frequently occur [30].

Although studies have reported the injury risk for projectile impacts to the globe, none have reported the corresponding intraocular pressure. Traumatic glaucoma and cataracts have been linked with open- and closed-globe injury [31-35]. Quantifying intraocular pressure during impacts may provide insight into these vision problems. Therefore, the purpose of the current study is to determine intraocular pressure during high speed projectile impacts to eyes.

**Methods**

Blunt impacts to porcine eyes were performed using a custom impact system designed and built to determine intraocular pressure. The test setup consisted of a pneumatically powered cannon with a pressure regulator to control projectile velocity, a solenoid valve, and three changeable barrels (Figure 1). To ensure a direct hit to the cornea, a placement guide was constructed to support, but not constrain movement, of the eye. Previous research showed that ocular muscles do not affect the impact at high dynamic rates [36-38]. In preparation for testing, porcine eyes were connected with a needle to a water chamber filled to produce an initial intraocular pressure of 14.95 mmHg (8 in$H_2O$) to represent normal physiologic pressure. The optic nerve and needle were secured with a clamping system.

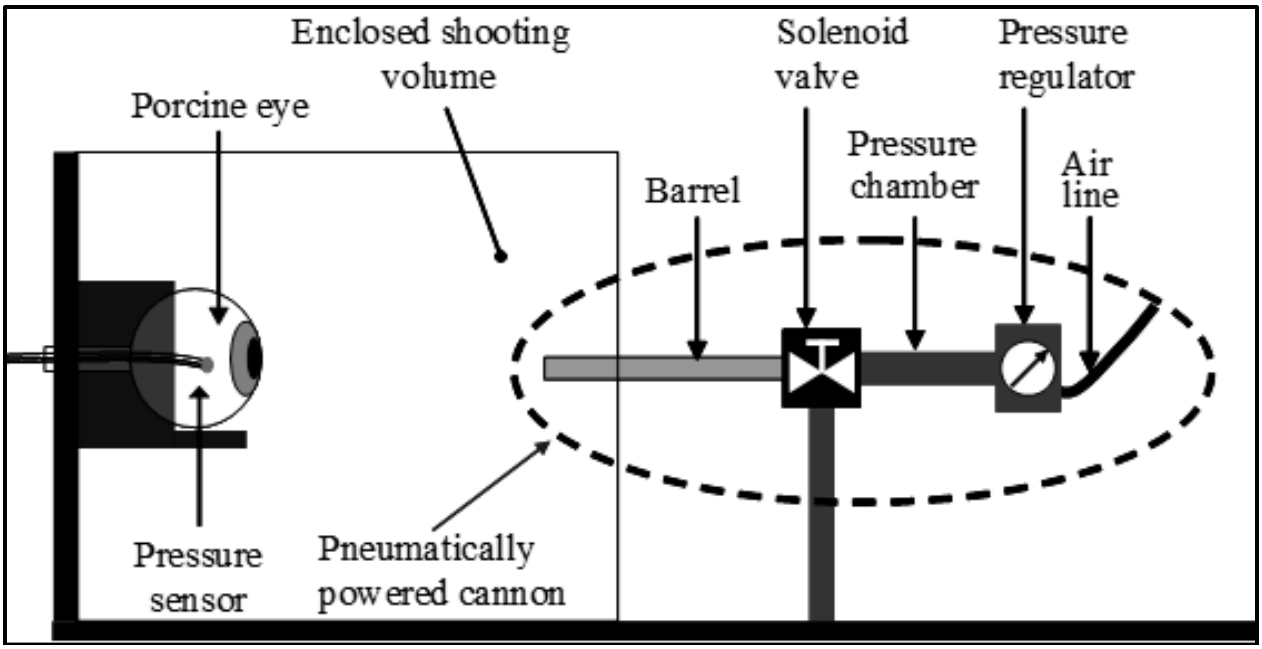


**Figure 1.** Experimental testing was performed using a pneumatically powered cannon in an enclosed shooting volume to impact porcine eyes.

Twelve porcine eyes were procured from Animal Technologies (Tyler, TX) and stored in saline for the current test series. Porcine donors were approximately six months of age at time of slaughter. Eyes were refrigerated for a maximum of 14 days before testing. Because tissue was never exposed to a freeze-thaw cycle and was stored in refrigerated saline, the integrity of the globe was preserved prior to testing. A previous study showed lack of correlation between rupture pressure and the time from harvest to test date ($R^2$=0.06) [4].

Intraocular pressure measurements were acquired using an in situ pressure sensor. This small pressure sensor (Precision Measurement Company, Model 060, Ann Arbor, MI) was inserted in the eye through the optic nerve [39]. The pressure transducer was rated for a range of 0-25877 mmHg (0-500 psi) and had a frequency response of 10 kHz which were both sufficient for this application. Given the incompressible nature in the eye, the effect of varied location of the pressure sensor inside the eye was not a factor. A previous study inserted multiple sensors into a single eye to compare the response of two identical pressure sensors in different locations during a dynamic event [23-26]. The response showed that pressure output was identical regardless of location.

A total of 36 tests were performed on 12 porcine eyes with a range of velocities between 6.2 m/s and 66.5 m/s. Projectiles selected for the test series included a 6.35 mm diameter metal ball, a 9.25 mm diameter aluminum rod, and an 11.16 mm diameter aluminum rod (Figure 2). For each test, the barrel size was chosen and the pressure regulator set to produce the desired velocity. A Phantom v9.1 camera (Vision Research, Wayne, NJ) captured video at 3902 frames per second with a resolution of 960 x 480, and the data acquisition system (DAS) collected data at 50 kHz. The pressure sensor measured intraocular pressure throughout the event and was filtered using channel frequency class 3500 Hz.

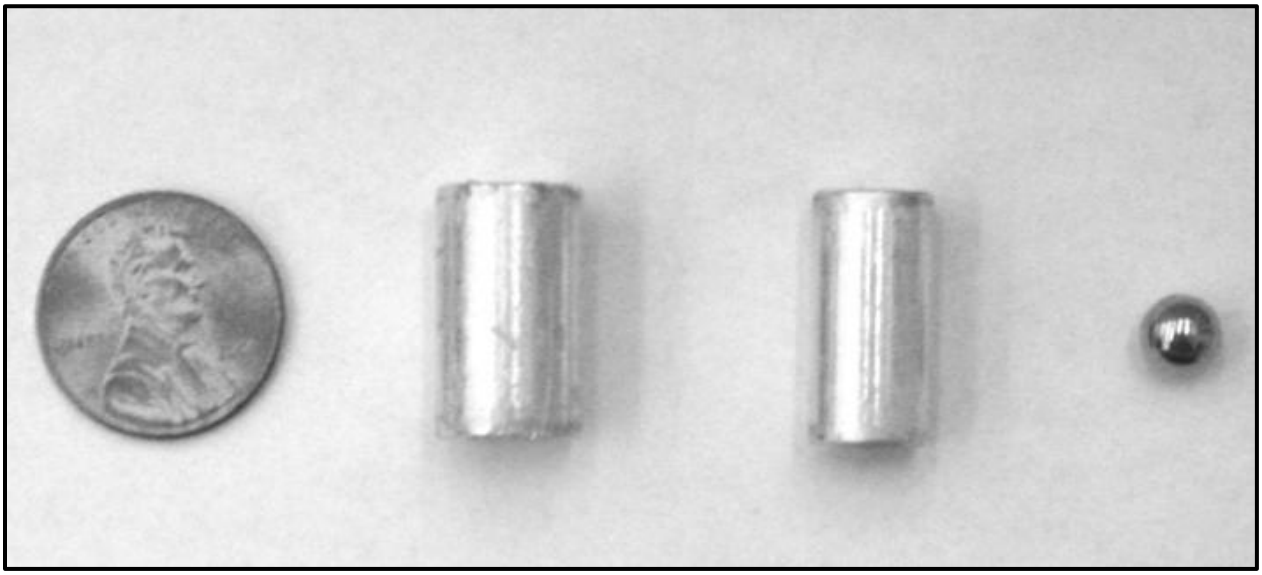

**Figure 2.** Relative sizes of the three projectiles compared to a penny (Left to Right: penny, 11.16 mm diameter aluminum rod, 9.25 mm diameter aluminum rod, 6.35 mm diameter metal ball).

High speed video was used to track the velocity of each projectile impact. Normalized energy is defined as the kinetic energy divided by the cross-sectional area of the object. This calculation included object mass (m), velocity (v), and cross-sectional area (A) [20]. Projectile velocity, normalized energy and intraocular pressure were reported for each test. Eyes were examined between each test to ensure integrity.

**Results**

A total of 36 projectile impact tests on 12 porcine eyes were conducted that produced a range of intraocular pressures representative of a variety of eye injury severities. Intraocular pressures ranged between 2041 mmHg to 26418 mmHg (39 psi - 511 psi) depending on projectile speed

and size. Normalized energy levels varied between 1016.2 J/m$^2$ and 71262.2 J/m$^2$. Projectile velocities ranged between 6.2 m/s and 66.5 m/s (Figure 3). Intraocular pressure, normalized energy, and velocity for each test were recorded (Tables 1-3). Four tests resulted in globe rupture.

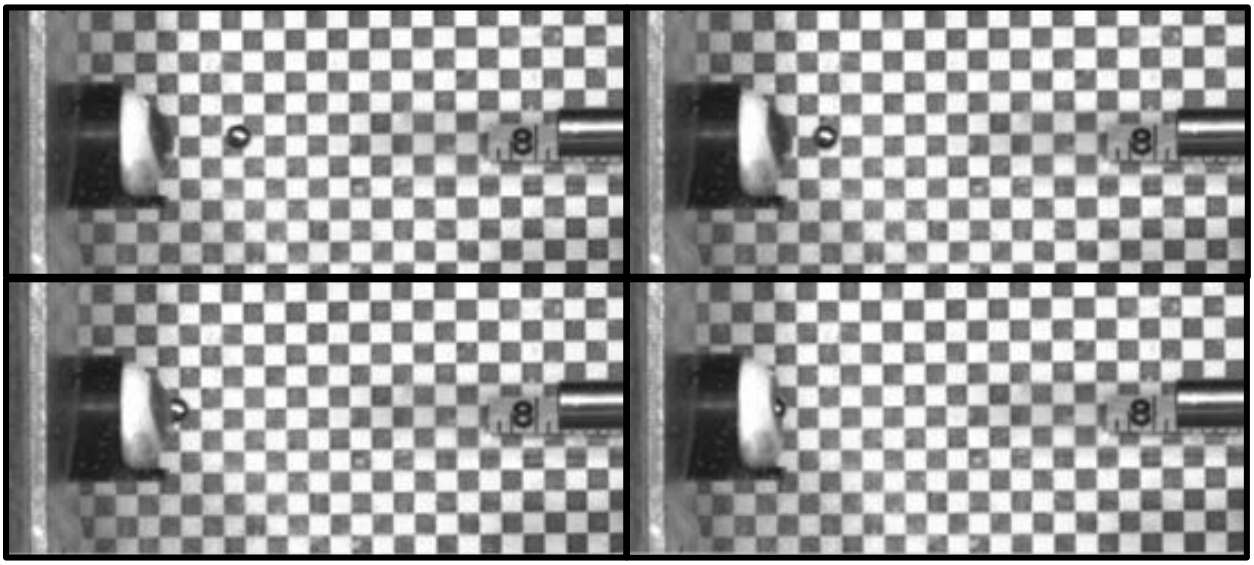

**Figure 3.** High speed video documentation of a test with the 6.35 mm diameter metal ball.

**Table 1.** Velocity, intraocular pressure, and normalized energy results for the small aluminum rod projectile (mass = 3.61 g, diameter = 9.25 mm).

| Small Aluminum Rod Projectile | | | | | |
|---|---|---|---|---|---|
| | Eye | Velocity (m/s) | Intraocular Pressure | | Normalized Energy* (J/m$^2$) |
| | | | (psi) | (mmHg) | |
| 1 | 1 | 7.6 | 53.4 | 2760.8 | 1552.7 |
| 2 | 2 | 23.6 | 382.2 | 19763.8 | 14999.3 |
| 3 | 2 | 35.0 | 497.2 | 25713.4 | 32813.3 |
| 4 | 11 | 7.9 | 77.0 | 3980.1 | 1666.6 |
| 5 | 11 | 18.0 | 247.2 | 12781.6 | 8741.1 |
| 6 | 11 | 24.8 | 367.5 | 19007.7 | 16526.1 |
| 7** | 11 | 31.6 | 401.9 | 20782.4 | 26769.6 |
| 8 | 12 | 24.8 | 367.9 | 19028.4 | 16526.1 |
| 9 | 12 | 19.2 | 278.4 | 14396.8 | 9867.9 |
| 10 | 12 | 15.7 | 185.7 | 9606.0 | 6640.4 |
| 11 | 12 | 6.7 | 75.5 | 3904.6 | 1219.7 |
| 12** | 12 | 33.8 | 497.6 | 25731.1 | 30730.4 |

*Normalized Energy = Kinetic Energy / Projected Area, **Rupture

**Table 2.** Velocity, intraocular pressure, and normalized energy results for the large aluminum rod projectile (mass = 5.19 g, diameter = 11.16 mm).

| Large Aluminum Rod Projectile | | | | | |
|---|---|---|---|---|---|
| | Eye | Velocity (m/s) | Intraocular Pressure | | Normalized Energy* ($J/m^2$) |
| | | | (psi) | (mmHg) | |
| 1 | 7 | 7.3 | 109.0 | 5638.4 | 1424.8 |
| 2 | 8 | 24.8 | 423.2 | 21883.6 | 16322.5 |
| 3 | 8 | 11.2 | 159.5 | 8246.7 | 3346.2 |
| 4 | 9 | 11.3 | 170.3 | 8808.9 | 3372.4 |
| 5 | 9 | 18.0 | 302.9 | 15663.7 | 8633.4 |
| 6** | 9 | 24.7 | 510.8 | 26418.4 | 16195.7 |
| 7 | 10 | 12.9 | 188.4 | 9740.5 | 4442.7 |
| 8 | 10 | 6.2 | 91.9 | 4755.1 | 1016.2 |
| 9 | 10 | 16.8 | 304.7 | 15756.0 | 7529.0 |
| 10 | 10 | 24.8 | 495.8 | 25637.7 | 16322.5 |

*Normalized Energy = Kinetic Energy / Projected Area, **Rupture

**Table 3.** Velocity, intraocular pressure, and normalized energy results for the metal BB projectile (mass = 1.02 g, diameter = 6.35 mm).

| Metal BB | | | | | |
|---|---|---|---|---|---|
| | Eye | Velocity (m/s) | Intraocular Pressure | | Normalized Energy* ($J/m^2$) |
| | | | (psi) | (mmHg) | |
| 1 | 3 | 9.6 | 39.5 | 2040.5 | 1479.1 |
| 2 | 3 | 29.3 | 200.4 | 10361.1 | 13838.9 |
| 3 | 3 | 42.8 | 318.9 | 16490.8 | 29561.2 |
| 4 | 3 | 50.7 | 404.2 | 20903.5 | 41455.3 |
| 5 | 3 | 59.8 | 472.1 | 24413.7 | 57505.2 |
| 6 | 4 | 20.3 | 118.7 | 6140.8 | 6632.8 |
| 7 | 4 | 29.3 | 202.7 | 10484.5 | 13838.9 |
| 8 | 4 | 42.8 | 380.5 | 19679.5 | 29561.2 |
| 9** | 4 | 66.5 | 431.1 | 22295.9 | 71262.2 |
| 10 | 5 | 32.7 | 201.2 | 10407.4 | 17216.7 |
| 11 | 5 | 42.8 | 312.0 | 16135.9 | 29561.2 |
| 12 | 5 | 20.3 | 133.6 | 6907.8 | 6632.8 |
| 13 | 5 | 51.9 | 397.7 | 20565.9 | 43318.2 |
| 14 | 6 | 41.6 | 441.2 | 22816.5 | 27808.2 |

*Normalized Energy = Kinetic Energy / Projected Area, **Rupture

## Discussion

This study investigates the correlation between intraocular pressure and kinetic energy and intraocular pressure and normalized energy. A strong nonlinear correlation between intraocular pressure and kinetic energy was observed for all tests ($R^2$=0.88) (Figure 4). A weaker nonlinear

correlation between intraocular pressure and normalized energy was observed for all tests ($R^2$=0.52). Overall, kinetic energy shows better correlation for all points than normalized energy. Three separate correlation curves are presented for intraocular pressure and normalized energy, one for each projectile (Figure 5). When separated by projectile type, there is a higher correlation between intraocular pressure and normalized energy than intraocular pressure and kinetic energy for both cylinders. Previously, it was determined that normalized energy was the most significant predictor of injury [20]. The current study suggests kinetic energy is a better predictor of pressure when projectile dimensions are unknown.

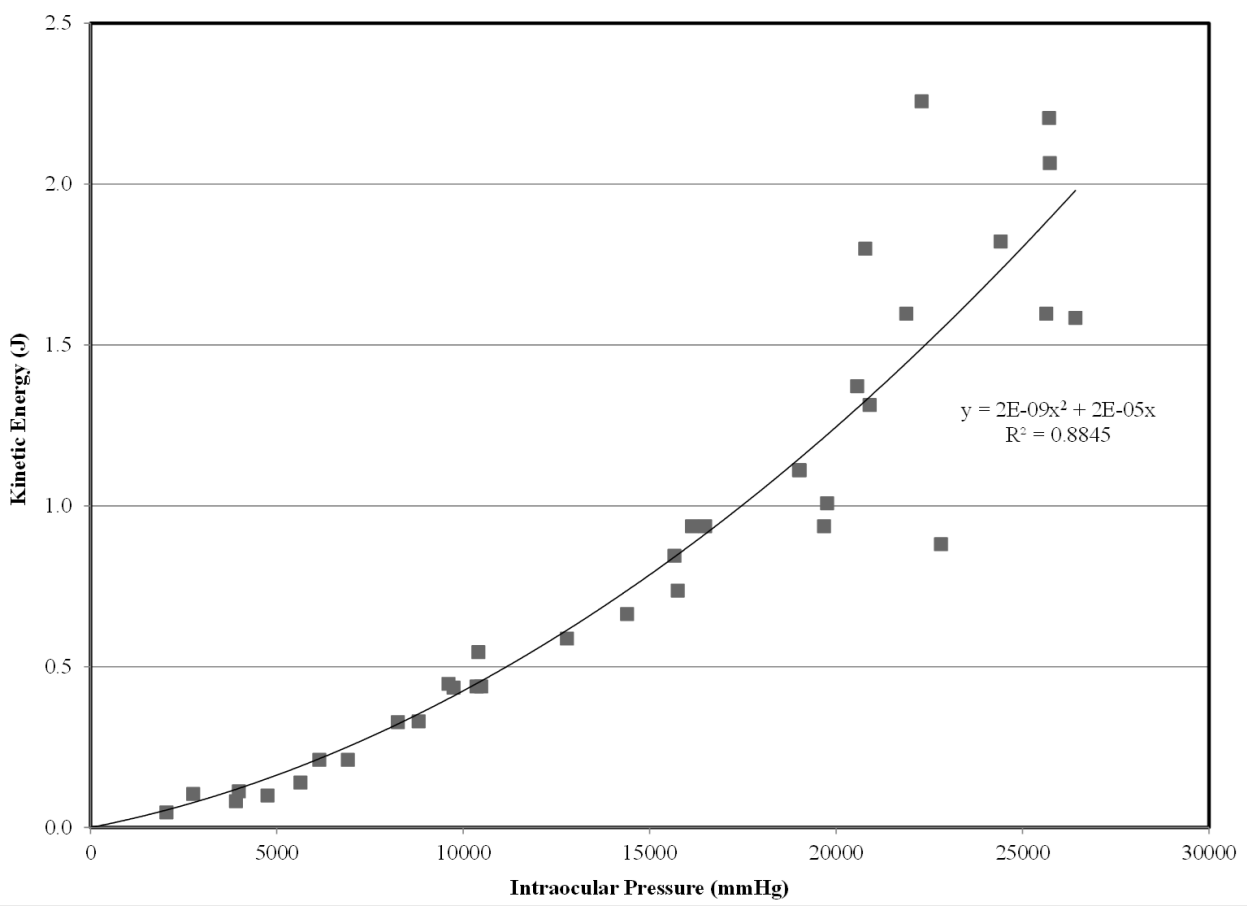


**Figure 4.** Correlation between intraocular pressure and kinetic energy for all tests.

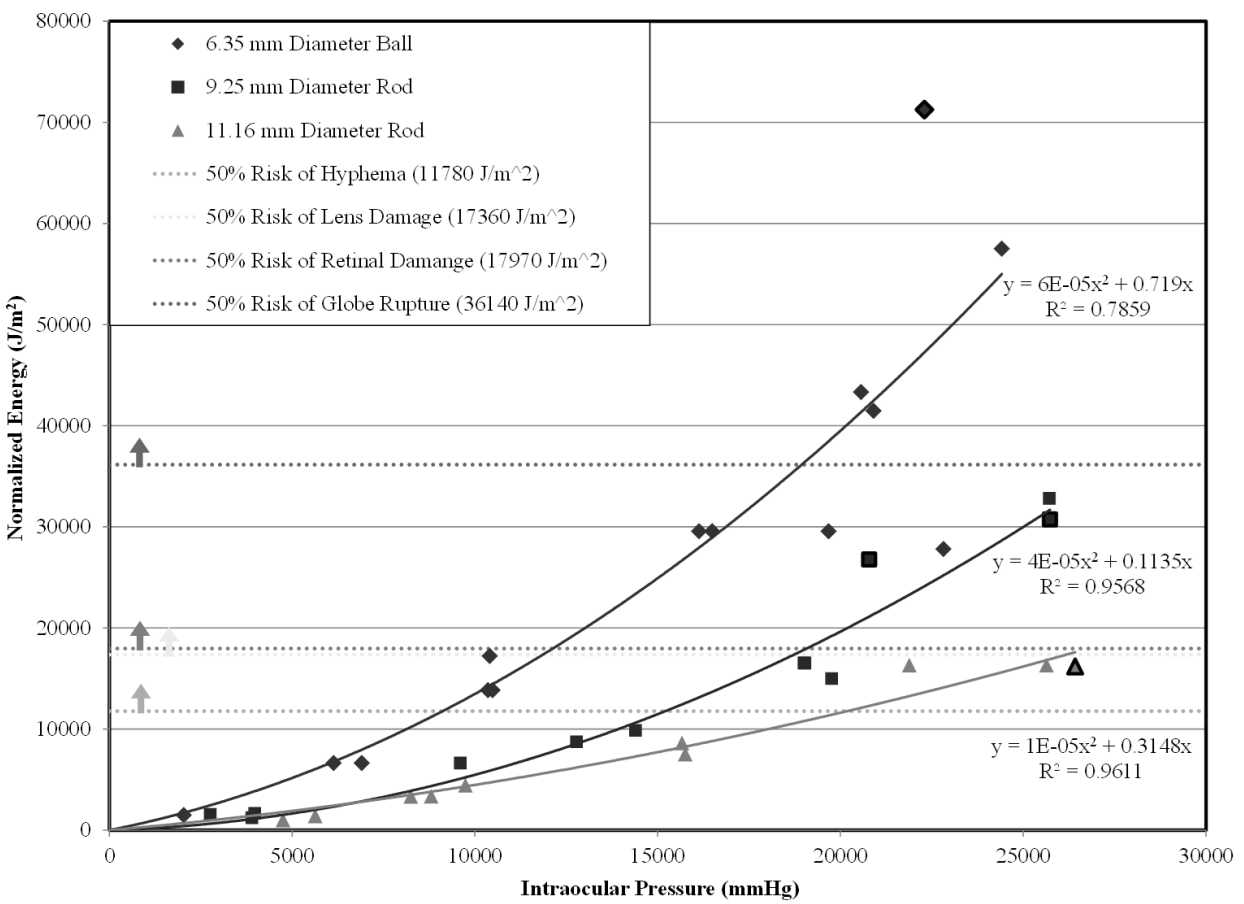


**Figure 5.** Correlation between intraocular pressure and normalized energy for each projectile type with 50% risk of four human ocular injuries. Circled points denote globe rupture. "y" represents normalized energy in joules per square meter associated with an intraocular pressure of "x" mmHg.

Projectile velocities tested in this study are within the range of consumer products greater than velocities from foam dart guns and below those from airsoft and paintball guns [15, 41]. Data from this study show that the risk of acute ocular injury from the tested projectiles and velocities is low; however, it is possible that the measured pressures may indicate delayed onset of ocular complications such as glaucoma and cataracts [31-35]. These underlying complications of ocular trauma may go unnoticed and untreated until they have progressed severely [31]. The correlations between intraocular pressure and energy, both kinetic and normalized, presented in this study have potential to be used in future applications including computational models of the eye and instrumented synthetic eyes for an advanced anthropomorphic head that can measure intraocular pressure during impacts [40-44].

The use of porcine eyes as a surrogate for human eyes was a limitation in this study; however, due to the anatomical similarities between porcine and human eyes, porcine eyes are a reasonable surrogate. Bisplinghoff et al. reported an average human intraocular rupture pressure as 7275 mmHg (141 psi) with a maximum pressure of 11925 mmHg (231 psi) [23], and Kennedy et al. reported an average porcine intraocular rupture pressure of 12256 mmHg (237 psi) with a maximum pressure of 16342 mmHg (316 psi) [4, 23-26]. There were 24 impacts that exceeded the average human intraocular rupture pressure and of these, 17 that exceeded the average porcine intraocular rupture pressure, but did not rupture. There were 3 impacts that exceeded the normalized energy 50% risk of human globe rupture that did not rupture. The boundary conditions and short impact duration help explain the lack of rupture. The apparatus that fixed the eye in place for a test constrained equatorial expansion, which resulted in higher intraocular pressures as the eye expansion was restricted. Furthermore, it is likely that very short duration (approximately 0.5 ms) of the impacts did not allow sufficient time for stress to develop in the tissues. Similar conditions should be placed on future work to ensure congruence between the data presented and new data.

The use of cadaveric tissue is another limitation in this study. Eye vasculature was not perfused for testing and therefore hemorrhage could not be studied. A future model may include an eye that has vascular pressure in order to study the specific effects related to chronic ocular injuries. Future work related to the current study could investigate the effect of off-center impacts to the eye, as the current study considers only direct impacts to the cornea.

Additionally, the effect of wearing different types of eyeglasses or protective eyewear could be studied to quantify the degree to which these protect against ocular injuries in the event of impact. Data from this could aid in redesign of current products or suggest that regular eyewear does not offer similar protective ability as specified protective eyewear.

For impact situations where normalized energy of the striking object is unavailable or not possible to calculate, this study illustrates the use of intraocular pressure for the determination of associated eye injury risk. Results from this study can provide foundation data for the design of safe consumer products from acute injury, as well as providing insight into chronic eye disease.

# Chapter 3:
# Eye Injury Risk from Water Stream Impact: Biomechanically Based Design Parameters for Water Toy and Park Design


## Abstract

**Purpose:** Interactive water displays are becoming increasingly popular and can result in direct eye contact. Therefore, the purpose of this study is to investigate eye injury risk from high speed water stream impacts and to provide biomechanically based design parameters for water toys and water park fountains.

**Methods:** An experimental matrix of 38 tests was developed to impact eight porcine eyes with water streams using a customized pressure system. Two stream diameters (3.2 mm and 6.4 mm) were tested at water velocities between 3.0 m/s and 8.5 m/s. Intraocular pressure was measured with a small pressure sensor inserted through the optic nerve and used to determine the injury risk for hyphema, lens dislocation, retinal damage, and globe rupture for each impact.

**Results:** Experimental water stream impacts created a range of intraocular pressures between 3156 mmHg and 7006 mmHg (61 psi to 135 psi). Injury risk varied between 4.4% - 27.8% for hyphema, 0.0% - 3.0% for lens dislocation, and 0.1% - 3.3% for retinal damage. All tests resulted in 0.0% injury risk for globe rupture. The two water stream diameters did not result in significantly different water stream velocities ($p = 0.32$); however, the variation in water stream diameter did result in significantly different intraocular pressures ($p = 0.03$), with higher pressures for the 6.4 mm stream.

**Conclusions:** This is the first study to experimentally measure intraocular pressure from high speed water stream impacts and quantify the corresponding eye injury risk. It is recommended that toy water guns and water park fountains use an upper threshold of 8.5 m/s for water stream velocities to prevent serious eye damage from impacts.



**Keywords:** Eye injury, Intraocular pressure, Water stream, Water fountain, Water toy


## Introduction

Each year approximately 2 million people in the United States suffer eye injuries that require treatment [1]. The most common sources of eye injuries include automobile accidents [2-10, 13, 14], sports related impacts [13, 14], military combat [16], and consumer products. These events result in nearly 500,000 cases of lost eyesight in the United States each year [17]. In addition to

affecting quality of life, the injuries are expensive to treat given the estimated annual cost associated with adult vision problems in the United States of $51.4 billion [18, 19].

Recently, there has been a dramatic increase in the popularity of water toys and recreational water parks that utilize pressurized water streams. Examples of these pressurized water streams that may pose a risk of ocular injury are interactive water fountains, water toys, and squirt guns. Water park attractions typically feature synchronized water streams directed vertically from the ground. Current regulations focus on filtration systems and prevention of bacterial spread, and distract attention from potential mechanical ocular injuries. Stream size and velocity are a critical part of the performance of such a fountain; however, it is currently impossible to place quantitative guidelines on their design without knowing the relationships between these factors and eye injury risk. With increasing consumer interest, there are competitive pressures to increase the performance of these devices, thereby increasing the pressure and velocity of the water streams.

While studies of water-induced ocular injuries have not been conducted on human eyes, high velocity water streams have been linked to ocular damage in agricultural animal studies. Fish (*Oncorhynchus tshawytscha*) exposed to submerged water streams with velocities between 12 m/s and 20 m/s were examined for injury. Nearly half suffered eye injuries (bulged, hemorrhaged, or missing) at velocities greater than 17 m/s [45]. In a similar study, velocity was determined to be positively correlated to severity of injury for fish released at velocities up to 21 m/s [46]. No current studies exist that examine the risk of human eye injuries from water streams up to 8.5 m/s, which is the primary design range for consumer products.

To predict and prevent eye injuries for various impact scenarios, previous research investigated eye injuries for projectile impacts with known projectile characteristics [13, 20, 21]. Duma et al. studied diameter, mass, velocity, kinetic energy, and normalized energy to determine the best ocular injury predictor [20]. A logistic regression analysis concluded that normalized energy was the most significant predictor of injury type and tissue lesion. Kennedy reported values for human 50% injury risk of corneal abrasion, lens dislocation, hyphema, retinal damage, and globe rupture [22]. This presented useful for predicting eye injuries given known projectile characteristics. However, there are many cases of blunt trauma where these variables are unknown and the measurement of intraocular pressure is useful.

Previous studies used intraocular pressure to determine the rupture pressure for the human eye [23, 24]. Intraocular pressure was dynamically induced within the eye and measured by a small pressure sensor inserted through the optic nerve. High rate pressurization resulted in a mean rupture pressure of 7275 ± 2175 mmHg (141 ± 42.1 psi) [23, 24]. Other studies show lower values for quasi-static loading [27-29]. These studies provide pressure results for the most severe eye injuries, but additional data is needed to represent the less severe injuries that frequently occur [30].

Traumatic glaucoma and cataracts have been linked with open and closed globe injuries [31-35]. Quantifying intraocular pressure during impacts will provide additional insight to these vision problems. Therefore, the purpose of this study is to quantify injury risk of hyphema, lens dislocation, retinal damage, and globe rupture associated with water jets of common stream sizes with velocities up to 8.5 m/s. This data will provide necessary information to create appropriate regulations for increasingly popular water fountains and toys.

**Methods**

*Test Setup:* Water impact tests were performed using a custom fluid system designed and built to determine intraocular pressure. The test setup consisted of a pressure tank with a regulator to control water velocity, a solenoid valve, and two changeable barrels (Figure 6). To ensure a direct corneal impact, a placement guide was constructed to support but not constrain movement of the eye. Previous research showed that ocular muscles do not affect impacts at high dynamic rates [36]. In preparation for testing, eyes were connected with a needle to a water chamber filled to produce an initial intraocular pressure of 14.95 mmHg (8 in$H_20$) to represent normal physiologic pressure. The optic nerve, needle, and pressure sensor were secured with a clamping system.

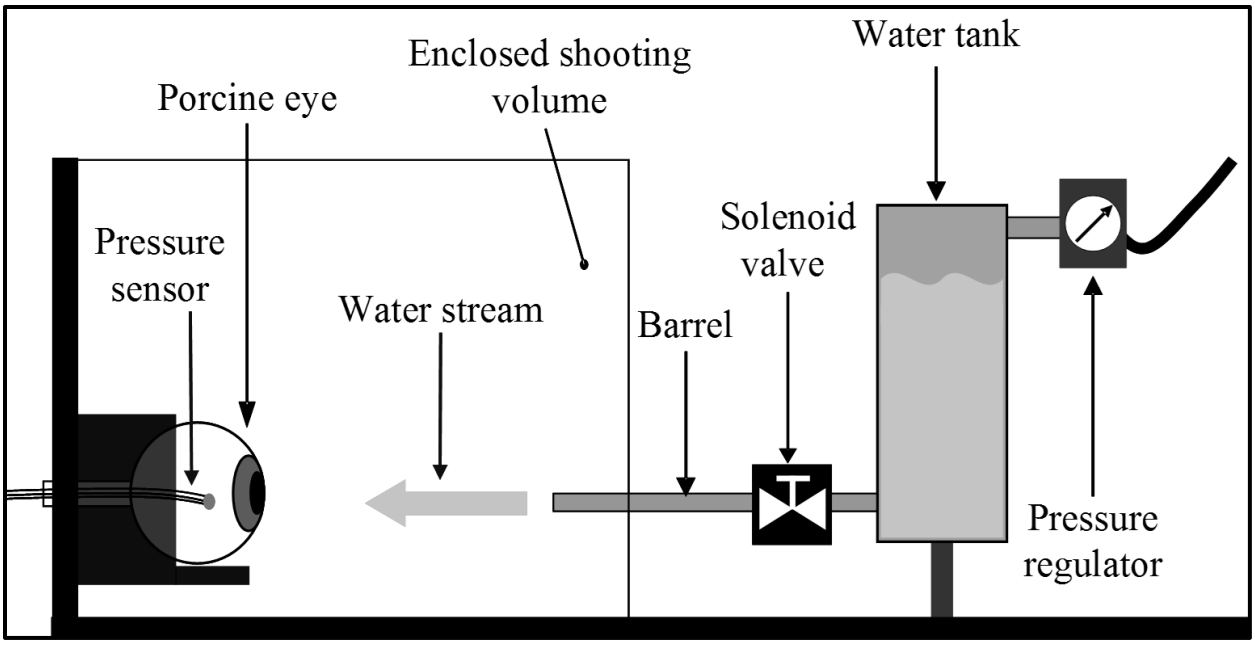


**Figure 6.** Water stream system used to impact porcine eyes.

Eight porcine eyes were procured from Animal Technologies (Tyler, TX) and stored in saline for the current test series. Porcine donors were approximately six months of age at time of slaughter. Eyes were refrigerated for a maximum of 14 days before testing. Because tissue was never exposed to a freeze-thaw cycle but rather was stored in refrigerated saline, globe integrity was preserved prior to testing. A previous study showed lack of correlation between rupture pressure and the time from harvest to test date ($R^2$=0.06) [4]. Eyes were examined between each test to ensure integrity.

Intraocular pressure measurements were acquired using an *in situ* pressure sensor. This small pressure sensor (Precision Measurement Company, Model 060, Ann Arbor, MI) was inserted in the eye through the optic nerve [23]. This pressure transducer was rated for a range of 0-25857 mmHg (0-500 psi) and had a frequency response of 10 kHz which were both sufficient for this application. Given the incompressible nature in the eye, the effect of varied location of the pressure sensor inside the eye was not a factor. A previous study inserted multiple sensors into a single eye to compare the response of two identical pressure sensors in different locations during a dynamic event [23, 24]. The response showed that pressure output was identical regardless of location.

A total of 38 tests were performed on 8 porcine eyes with a range of velocities between 3.0 m/s and 8.5 m/s. Water streams selected for the test series had barrel diameters of 3.2 mm and 6.4 mm. For each test, the barrel size was chosen and the pressure regulator set to produce a desired velocity. A Phantom v9.1 camera (Vision Research, Wayne, NJ) captured video at 3902 frames per second with a resolution of 960 x 480, while a data acquisition system collected data at 50 kHz. The pressure sensor measured intraocular pressure throughout the event and was filtered using channel frequency class 3500 Hz. High speed video was used to track the velocity of each projectile impact.

*Correlation of Intraocular Pressure to Injury Risk:* Duma et al. previously determined second-degree polynomial equations that correlate intraocular pressure to normalized energy for three rigid projectiles of diameters 6.35 mm, 9.25 mm, and 11.16 mm [47]. These equations relate intraocular pressure 'x' (mmHg) to normalized energy 'y' (J/m$^2$). Normalized energy for the water stream impacts was calculated using the equation for the smallest projectile (6.35 mm diameter) due to its similarity to both stream diameters **Equation 1**.

$$y = 6e^{-5}x^2 + 0.719x \quad R^2 = 0.7859 \qquad \textbf{Equation 1}$$

Injury risk as a function of normalized energy was previously determined for ocular injuries (Eq. 2) [21]. This equation was used to determine injury risk for hyphema, lens dislocation, retinal damage, and globe rupture for all 38 tests. In **Equation 2**, 'x' is normalized energy in J/m$^2$. The scale (α) and shape (β) parameters for hyphema are 14233.2 and 1.94012, for lens dislocation are 19012.0 and 4.03800, for retinal damage are 19826.3 and 3.73625, and for globe rupture are 38524.9 and 5.73194, respectively.

$$Injury\ Risk = \left[1 - e^{-(x/\alpha)^{\beta}}\right] * 100\% \qquad \textbf{Equation 2}$$

*Statistical Analysis:* A two-sample t-test assuming unequal variances was performed to compare the velocity of all tests between both diameter sizes. A similar test was performed to compare resulting intraocular pressure.

## Results

High speed video provided measurement of water velocity, which ranged between 3.0 m/s and 8.5 m/s (Figure 7). There was no observed relationship between water velocity and intraocular pressure for the 3.2 mm diameter ($R^2 = 0.05$) or the 6.4 mm diameter ($R^2 = 0.02$) streams for the range of velocities tested (Figure 8). The average velocity was 5.3 ± 1.7 m/s for the 3.2 mm diameter water stream and 4.8 ± 1.3 m/s for the 6.4 mm diameter water stream. Velocities of the 3.2 mm and 6.4 mm diameter streams were not significantly different ($p = 0.32$).

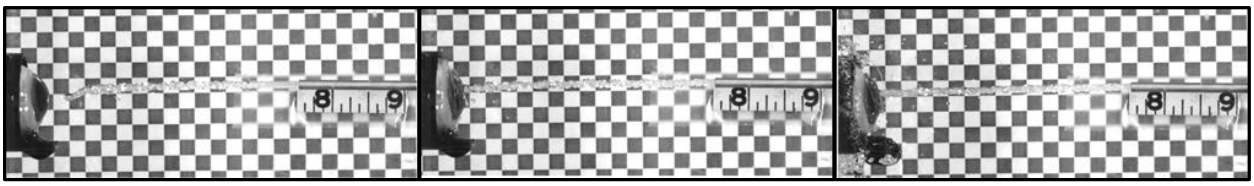

**Figure 7.** High speed video documentation of a test with a 3.2 mm water stream at 4.1 m/s. (Left) Water stream prior to impact. (Middle) Water stream upon impact. (Right) Water stream during impact.

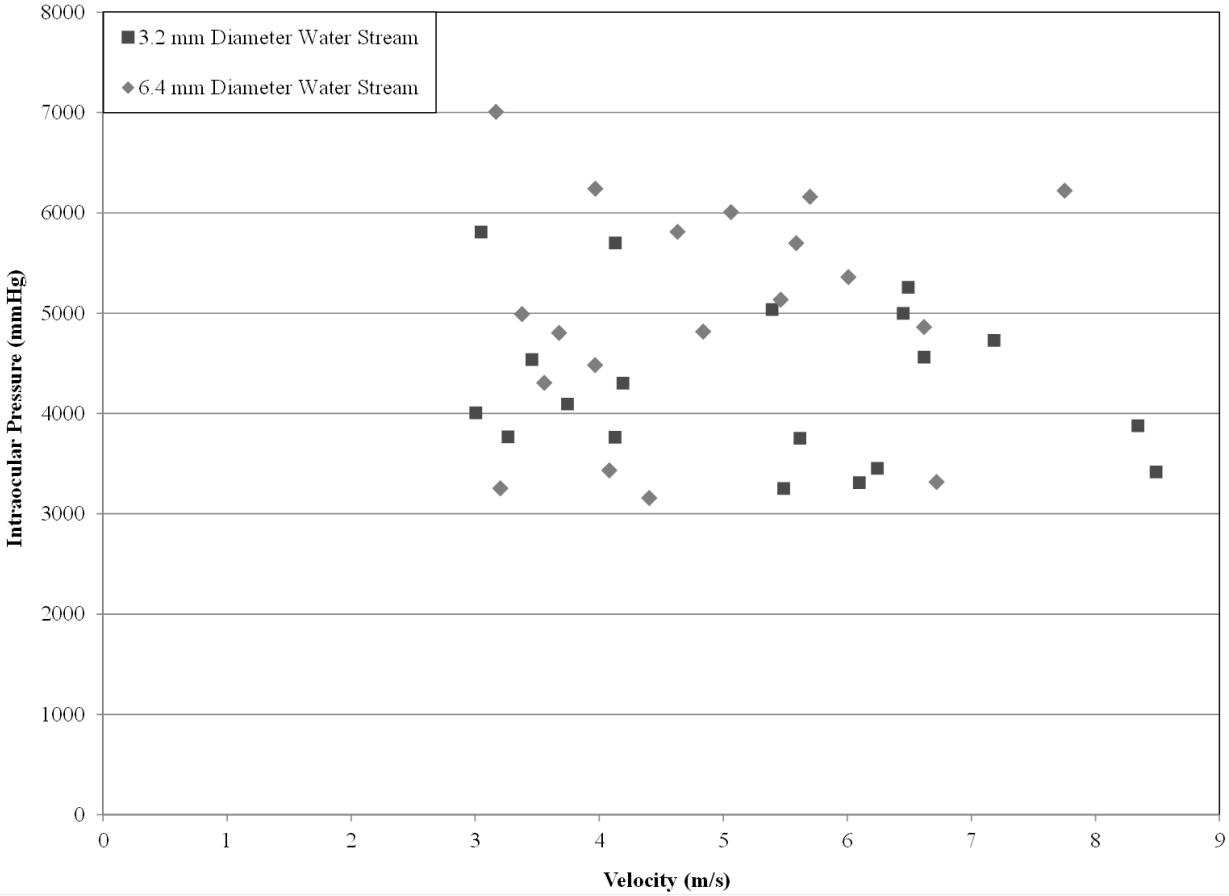


**Figure 8.** Relationship between intraocular pressure and stream velocity for the two water stream diameters.

The pressure transducer measured intraocular pressures between 3156 mmHg and 7006 mmHg (61 psi to 135 psi). The average intraocular pressure was 4295.0 ± 790.5 mmHg (83.1 ± 15.3 psi) for the 3.2 mm diameter water stream and 5002.5 ± 1137.5 mmHg (96.7 ± 22.0 psi) for the 6.4 mm diameter water stream. Pressure for the 3.2 mm diameter water stream was significantly lower ($p = 0.03$) than pressure of the 6.4 mm diameter water stream.

Corresponding normalized energy levels varied between 2867.24 $J/m^2$ and 7982.77 $J/m^2$ and correspond to injury risk between 4.4% - 27.8% for hyphema, 0.0% - 3.0% for lens dislocation, and 0.1% - 3.3% for retinal damage. All tests resulted in 0.0% injury risk for globe rupture. Impacting velocity, resulting intraocular pressure, and normalized energy as well as the injury risk for hyphema, lens damage, retina damage, and globe rupture were recorded and calculated for each test (Tables 4, 5).

**Table 4.** Velocity, intraocular pressure, normalized energy, and injury risk for hyphema, lens dislocation, retinal damage, and globe rupture for the 6.4 mm water stream diameter.

| 6.4 mm Diameter | | | | | | | | | |
|---|---|---|---|---|---|---|---|---|---|
| Test | Eye | Velocity (m/s) | Intraocular Pressure (psi) | Intraocular Pressure (mmHg) | Normalized Energy ($J/m^2$) | % Injury Risk | | | |
| | | | | | | Hyphema | Lens Dislocation | Retinal Damage | Globe Rupture |
| 1 | 1 | 6.72 | 64.14 | 3316.76 | 3044.81 | 4.9 | 0.1 | 0.1 | 0.0 |
| 2 | 1 | 4.08 | 66.36 | 3431.83 | 3174.13 | 5.3 | 0.1 | 0.1 | 0.0 |
| 3 | 1 | 3.20 | 62.90 | 3252.62 | 2973.41 | 4.7 | 0.1 | 0.1 | 0.0 |
| 4 | 1 | 4.40 | 61.03 | 3156.41 | 2867.24 | 4.4 | 0.0 | 0.1 | 0.0 |
| 5 | 2 | 3.56 | 83.23 | 4304.44 | 4206.59 | 9.0 | 0.2 | 0.3 | 0.0 |
| 6 | 2 | 3.68 | 92.86 | 4802.19 | 4836.43 | 11.6 | 0.4 | 0.5 | 0.0 |
| 7 | 2 | 4.63 | 112.33 | 5809.30 | 6201.77 | 18.1 | 1.1 | 1.3 | 0.0 |
| 8 | 2 | 5.46 | 99.28 | 5134.44 | 5273.42 | 13.6 | 0.6 | 0.7 | 0.0 |
| 9 | 2 | 6.01 | 103.63 | 5358.98 | 5576.23 | 15.0 | 0.7 | 0.9 | 0.0 |
| 10 | 3 | 4.84 | 93.13 | 4816.09 | 4854.45 | 11.7 | 0.4 | 0.5 | 0.0 |
| 11 | 3 | 5.70 | 119.10 | 6159.45 | 6704.98 | 20.7 | 1.5 | 1.7 | 0.0 |
| 12 | 3 | 6.62 | 94.01 | 4861.66 | 4913.68 | 11.9 | 0.4 | 0.5 | 0.0 |
| 13 | 3 | 3.38 | 96.50 | 4990.62 | 5082.63 | 12.7 | 0.5 | 0.6 | 0.0 |
| 14 | 3 | 3.97 | 86.64 | 4480.66 | 4426.17 | 9.9 | 0.3 | 0.4 | 0.0 |
| 15 | 4 | 5.59 | 110.17 | 5697.22 | 6043.80 | 17.3 | 1.0 | 1.2 | 0.0 |
| 16 | 4 | 7.75 | 120.30 | 6221.55 | 6795.76 | 21.2 | 1.6 | 1.8 | 0.0 |
| 17 | 4 | 3.17 | 135.48 | 7006.27 | 7982.78 | 27.8 | 3.0 | 3.3 | 0.0 |
| 18 | 4 | 3.97 | 120.65 | 6239.21 | 6821.66 | 21.3 | 1.6 | 1.8 | 0.0 |
| 19 | 4 | 5.06 | 116.17 | 6007.64 | 6485.00 | 19.6 | 1.3 | 1.5 | 0.0 |

**Table 5.** Velocity, intraocular pressure, normalized energy, and injury risk for hyphema, lens dislocation, retinal damage, and globe rupture for the 3.2 mm water stream diameter.

| 3.2 mm Diameter | | | | | | | | | |
|---|---|---|---|---|---|---|---|---|---|
| Test | Eye | Velocity (m/s) | Intraocular Pressure (psi) | Intraocular Pressure (mmHg) | Normalized Energy ($J/m^{2)}$ | % Injury Risk | | | |
| | | | | | | Hyphema | Lens Dislocation | Retinal Damage | Globe Rupture |
| 1 | 9 | 3.05 | 112.32 | 5808.38 | 6200.46 | 18.1 | 1.1 | 1.3 | 0.0 |
| 2 | 9 | 4.13 | 110.22 | 5699.79 | 6047.40 | 17.3 | 1.0 | 1.2 | 0.0 |
| 3 | 9 | 5.39 | 97.37 | 5035.29 | 5141.62 | 13.0 | 0.5 | 0.6 | 0.0 |
| 4 | 9 | 6.49 | 101.64 | 5256.15 | 5436.80 | 14.3 | 0.6 | 0.8 | 0.0 |
| 5 | 10 | 4.19 | 83.17 | 4300.95 | 4202.27 | 9.0 | 0.2 | 0.3 | 0.0 |
| 6 | 10 | 5.62 | 72.57 | 3752.76 | 3543.23 | 6.5 | 0.1 | 0.2 | 0.0 |
| 7 | 10 | 6.45 | 96.63 | 4997.35 | 5091.50 | 12.7 | 0.5 | 0.6 | 0.0 |
| 8 | 10 | 7.18 | 91.41 | 4727.39 | 4739.88 | 11.2 | 0.4 | 0.5 | 0.0 |
| 9 | 10 | 3.46 | 87.72 | 4536.41 | 4496.42 | 10.1 | 0.3 | 0.4 | 0.0 |
| 10 | 11 | 6.10 | 64.01 | 3310.04 | 3037.30 | 4.9 | 0.1 | 0.1 | 0.0 |
| 11 | 11 | 6.62 | 88.19 | 4560.51 | 4526.90 | 10.3 | 0.3 | 0.4 | 0.0 |
| 12 | 11 | 8.34 | 74.95 | 3875.90 | 3688.12 | 7.0 | 0.1 | 0.2 | 0.0 |
| 13 | 11 | 3.01 | 77.46 | 4005.81 | 3842.97 | 7.6 | 0.2 | 0.2 | 0.0 |
| 14 | 11 | 3.75 | 79.16 | 4093.88 | 3949.10 | 8.0 | 0.2 | 0.2 | 0.0 |
| 15 | 12 | 8.49 | 66.05 | 3415.66 | 3155.86 | 5.2 | 0.1 | 0.1 | 0.0 |
| 16 | 12 | 6.24 | 66.74 | 3451.42 | 3196.31 | 5.4 | 0.1 | 0.1 | 0.0 |
| 17 | 12 | 3.27 | 72.82 | 3766.08 | 3558.82 | 6.6 | 0.1 | 0.2 | 0.0 |
| 18 | 12 | 4.13 | 72.71 | 3760.38 | 3552.14 | 6.5 | 0.1 | 0.2 | 0.0 |
| 19 | 12 | 5.49 | 62.87 | 3251.45 | 2972.11 | 4.7 | 0.1 | 0.1 | 0.0 |

**Discussion**

This is the first study to document safe design parameters for water stream eye impacts. The data clearly show there is no risk of serious eye injuries such as globe rupture, retinal detachment, or lens dislocation for water velocities up to 8.5 m/s for either stream size tested. While there is some risk for hyphema, the data are varied depending on the specific porcine eye. Moreover, hyphema is a much less severe injury than the others as it typically resolves without complication or need for surgical intervention. Water stream impact case studies involving industrial pumps, agricultural irrigation equipment, and fire hoses do show eye injuries, but they occur at substantially higher water velocities. One case study involved an agricultural irrigation line with a water velocity of 28.96 m/s [48]. In this case, a farmer was struck with the water stream and received multiple lacerations and a severed artery in the eye. A second case involved an industrial pump line with water traveling at 182.9 m/s [49]. A man was tightening a leaking

pipe when it burst and hit him directly in the eye. His extraocular muscles were torn from the globe insertions and his eye was enucleated. These injuries are rare and occur with high water velocities in the range of 25 m/s to 200 m/s. When combined with the data presented in this paper, it is clear that water streams with velocities up to 8.5 m/s will not result in serious eye injury. Future work could investigate water streams at velocities between 8.5 m/s and 25 m/s which should provide a transition from no risk to serious eye injury. For now it is recommended that any water toy or water park not exceed 8.5 m/s water velocity.

The use of normalized energy was developed for rigid objects and requires projectile mass; however, the effective mass of a water stream is not comparable due to its deformable fluid nature. Therefore, normalized energy in this study is determined using the relationship of intraocular pressure and normalized energy of known rigid projectiles. Water stream diameters were matched as closely as possible to published projectile diameters to obtain the best correlation between intraocular pressure and normalized energy [22]. However, the smaller water stream is approximately half the diameter of the projectile and the resulting injury risks for this water stream may be underestimated.

The use of porcine eyes as a surrogate for human eyes was a limitation in this study because the porcine eye is thicker than the human eye. In previous literature, researchers used many surrogates for experimental testing [20]. Because of the anatomical and mechanical similarities between porcine and human eyes and because of their additional availability, porcine eyes were utilized for the current study. Additionally, a future model may include an eye with vascular pressure so as to study the specific effects related to chronic ocular injuries.

Data from this study show that the risk of acute ocular injury from the tested water velocities is low; however, it is possible that the measured pressures may indicate delayed onset of ocular complications such as glaucoma and cataracts [31-35]. These underlying complications of ocular trauma may go unnoticed and untreated until they have progressed severely [31]. Given that the physiological pressure of the eye is approximately 15 mmHg and the water streams resulted in pressures as high at 7005 mmHg, it is possible but unknown if chronic eye injuries may result. It is important to note that the duration of the peak pressures was extremely short, with peak values lasting far less than 1 ms. This extremely short duration does not impart enough energy for the stress in the tissues to result in rupture, even though some pressure values

are within the reported rupture range [21]. In order to rupture, high pressures would need to be maintained for nearly 10 ms. The data presented in this study have potential to be used in future applications including computational models of the eye and instrumented synthetic eyes for an advanced anthropomorphic head that can measure intraocular pressure during impacts [42-44, 50].

# Chapter 4:
# Eye Injury Risk Associated with Remote Control Helicopter Blades


## Abstract

Eye injuries can be caused by a variety of consumer products and toys. Recently, indoor remote controlled (RC) toy helicopters have become very popular. The purpose of this study is to quantify eye injury risk associated with five commercially available RC toy helicopter blades. An experimental matrix of 25 tests was developed to test five different RC toy helicopter blades at full battery power on six postmortem human eyes. A pressure sensor inserted through the optic nerve measured intraocular pressure. Corneal abrasion was assessed post-impact using fluorescein dye. Intraocular pressure was correlated to injury risk for hyphema, lens damage, retinal damage, and globe rupture using published risk functions. All tests resulted in corneal abrasions; however, no other injuries were observed. The 25 tests produced an increase intraocular pressure between 15.2 kPa and 99.3 kPa (114.3 mmHg and 744.7 mmHg). Calculated blade velocities ranged between 16.0 m/s and 25.4 m/s. Injury risk for hyphema was a maximum of 0.2%. Injury risk for lens damage, retinal damage, and globe rupture was 0.0% for all tests. Blade design parameters such as length and mass did not affect the risk of eye injury. This is the first study to quantify the risk of eye injury from RC toy helicopter blades. While corneal abrasions were observed, more serious eye injuries were neither observed nor predicted to have occurred. Results from this study are critical for establishing safe design thresholds for RC toy helicopter blades so that more serious injuries can be prevented.



**Keywords:** Eye Injury, Toy Helicopter, Corneal Abrasion


## Introduction

Each year approximately two million people in the United States suffer eye injuries that require treatment [1]. The most common sources of eye injuries include automobile accidents, sports impacts, military combat, and misuse of consumer products [14, 51]. Eye injuries affect quality of life and are expensive to treat, given an estimated annual cost of approximately $50 billion and nearly 500,000 years of lost eyesight in the United States [19, 17]. Traditionally, remote controlled (RC) toy helicopters were designed for outdoor use where large distances minimized the risk of eye contact. However, due to the increasing popularity of these toys and advances in inexpensive lightweight materials and batteries, RC toy helicopters have been redesigned for

indoor use. Indoor RC toy helicopters still have high velocity blades but can more readily navigate and hover at eye level, posing an increased risk of eye impact.

Previous research evaluated various impact scenarios in order to predict and prevent eye injuries. Duma et al. concluded that normalized energy is the most significant predictor of injury type and tissue lesion [20]. Kennedy and Duma reported normalized energy values associated with 50% injury risk for hyphema, lens damage, retinal damage, and globe rupture [22]. Intraocular pressure measurements were used to determine rupture pressure and material properties of the human eye [23]. Duma et al. correlated intraocular pressure to normalized energy to account for situations where projectile characteristics are unknown and normalized energy cannot be directly calculated [47]. Considering RC toy helicopter blade impacts, the characteristics required to calculate normalized energy are difficult to quantify and intraocular pressure measurement proves useful for evaluating eye injury risk. Therefore, the purpose of this study is to evaluate eye injury risk using intraocular pressure measurements for impacts between a variety of commercially available RC toy helicopter blades and human eyes.

**Methods**

Five battery-powered indoor RC toy helicopters were used to impact five of six postmortem human eyes for a total of 25 tests. The order of tests was randomized to ensure each helicopter impacted a new eye once. Helicopter blades were categorized as “fixed” or “free” depending on if they were segmented at the rotor. Blade length and mass were measured prior to testing (Table 6).

**Table 6.** Blade length, wingspan, and mass for all RC toy helicopters tested.

| RC Toy Helicopter Brand | Side View | Top View | Blade Length (cm) | Wingspan (cm) | Top Blade (mg) | Bottom Blade (mg) |
|---|---|---|---|---|---|---|
| Brookstone Chinook (free wing) |  |  | 6.6 | 15.3 | 637.9 | 653.9 |
| Brookstone Silver Bullet (free wing) |  |  | 5.6 | 12.4 | 828.5 | 667.7 |
| Playmaker Toys Flying Saucer (free wing) |  | 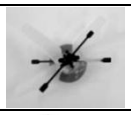 | 6.0 | 13.0 | 371.0 | 411.4 |
| Air Hogs Sharpshooter (fixed wing) |  | 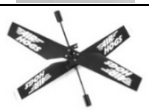 | - | 16.3 | 1649.4 | 1573.2 |
| BanDai Knight Flight Batman (fixed wing) |  |  | - | 17.0 | 1811.4 | 1996.9 |

Six postmortem human eyes were procured from the North Carolina Eye Bank (Winston-Salem, NC). The time between harvest and testing lacks correlation with rupture pressure ($R^2$ =0.06) [4]. Each eye was prepared one day prior to testing by inserting a miniature pressure transducer and a small tube through the optic nerve [23]. Eyes were covered with saline-soaked gauze to prevent drying and stored in a refrigerator overnight. A saline solution raised 20.3 cm above the eye was attached to the small tube using a 20 gage needle to provide an initial physiologic intraocular pressure of 2.0 kPa (14.9 mmHg). The effect of varied location of the pressure sensor within the globe was not a limiting factor given incompressibility of the eye [23]. Eyes were potted in synthetic orbits and surrounded by Knox gelatin to represent their *in vivo* location with respect to cranial bones and musculature. Previous research showed that ocular muscles do not affect impacts at high dynamic rates [36]. Eye integrity was preserved because tissue was never exposed to a freeze-thaw cycle. Prior to testing, fluorescein dye was applied to the eye. Dye was reapplied post-impact and viewed with a blue light for evidence of corneal abrasion. Helicopter batteries were charged and eyes were examined to ensure globe integrity between tests.

Intraocular pressure measurements were acquired at 20 kHz (TDAS PRO, DTS Inc., Seal Beach, CA) using a miniature pressure sensor (Precision Measurement Company, Model 060, Ann Arbor, MI) with a measurable range of 0 – 3447 kPa (0-25857 mmHg) and a frequency response of 10 kHz. Intraocular pressure was filtered using channel frequency class 3500 Hz. A Phantom v9.1 camera (Vision Research, Wayne, NJ) captured video at 2000 frames per second with a resolution of 512 x 320 pixels. High speed video was used to track blade movement and calculate blade velocity (**Figure 9**).

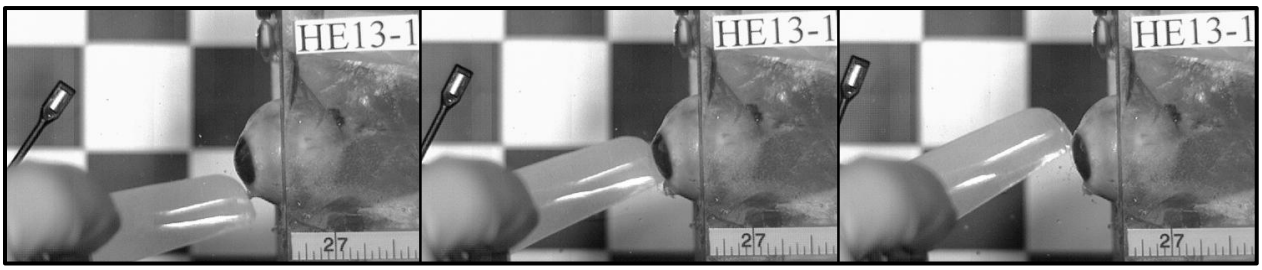


**Figure 9.** High speed video stills of impact of RC toy helicopter blade with human cadaver eye. (Left) Pre-impact. (Middle) During impact. (Right) Post-impact.

Equations that correlate intraocular pressure to normalized energy for three rigid projectiles were previously determined [47]. Normalized energy for the helicopter blades was calculated using the equation for the smallest tested projectile because its diameter (6.35 mm) is closest to the impacting surface area of the helicopter blade. Injury risk as a function of normalized energy was previously determined for eye injuries [22]. This relationship was used to determine injury risk for hyphema, lens dislocation, retinal damage, and globe rupture for all tests. Peak intraocular pressure and blade velocity was compared for each helicopter using a two-sample t-Test assuming unequal variance.

**Results**

No serious eye injuries were observed for any test. All tests resulted in minor corneal abrasions affecting less than 25% of the cornea. This effectively corresponds to the contact area of the blades with the eye. For all abrasions, only the epithelial layer of the cornea was affected as there were no observed lacerations.

The BanDai Knight Flight Batman intraocular pressure was significantly higher than Playmaker Toys Flying Saucer ($p=0.00$) intraocular pressure. The remaining intraocular pressures were not

significantly different (Table 7). The Brookstone Chinook blade velocity was significantly higher than the Air Hogs Sharpshooter (p=0.00) and BanDai Knight Flight Batman (p=0.00) blade velocities. The Brookstone Silver Bullet blade velocity was significantly higher than the Air Hogs Sharpshooter (p=0.00), BanDai Knight Flight Batman (p=0.00), and Playmaker Toys Flying Saucer (p=0.01). The remaining blade velocities were not significantly different (Table 7). Additionally, top blade impacts were not statistically different from bottom blade impacts with regard to impact velocity (p=0.78) or intraocular pressure (p=0.69). Free blade velocity was significantly higher than fixed blade velocity (p=0.00) but there was no significant difference between resulting intraocular pressures.

Blade velocity, intraocular pressure, normalized energy, and injury risk for hyphema, lens damage, retinal damage, and globe rupture are reported (Tables 8, 9). Intraocular pressures for the 25 tests ranged between 15.2 kPa to 99.3 kPa (114.3 mmHg to 744.7 mmHg). Normalized energy levels varied between 82.94 J/m$^2$ and 568.74 J/m$^2$. Blade impact velocities ranged between 16.0 m/s and 25.4 m/s. Maximum injury risk for hyphema was 0.2%, and there was 0.0% risk of lens damage, retinal damage, and globe rupture for all tests. There was no correlation between blade velocity and intraocular pressure. Blade mass was not correlated to pressure ($R^2$=0.20) or velocity ($R^2$=0.21). Blade length was not correlated with pressure ($R^2$=0.17) or velocity ($R^2$=.038).

**Table 7. Statistical analyses for intraocular pressure and blade velocities for each RC toy helicopter.**

| p-value | | Pressure | | | | |
|---|---|---|---|---|---|---|
| | | Air Hogs Sharpshooter | Bandai Knight Flight Batman | Brookstone Chinook | Brookstone Silver Bullet | Playmaker Toys Flying Saucer |
| Velocity | Air Hogs Sharpshooter | | 0.11 | 0.68 | 0.81 | 0.23 |
| | Bandai Knight Flight Batman | 0.77 | | 0.13 | 0.05 | 0.00 |
| | Brookstone Chinook | 0.00 | 0.00 | | 0.49 | 0.06 |
| | Brookstone Silver Bullet | 0.00 | 0.00 | 0.10 | | 0.31 |
| | Playmaker Toys Flying Saucer | 0.54 | 0.63 | 0.07 | 0.01 | |

**Table 8. Velocity, intraocular pressure, correlated normalized energy, and injury risk for free wing RC toy helicopters tested. 'T' indicates the top blade impact; "B" indicates the bottom blade impact.**

| Brookstone Chinook | | | | | | | | | |
|---|---|---|---|---|---|---|---|---|---|
| Eye | Blade | Velocity (m/s) | Intraocular Pressure (kPa) | Intraocular Pressure (mmHg) | Normalized Energy* ($J/m^2$) | % Injury Risk | | | |
| | | | | | | Hyphema | Lens Damage | Retinal Damage | Globe Rupture |
| 1 | T | 21.8 | 88.4 | 663.2 | 503.2 | 0.2 | 0.0 | 0.0 | 0.0 |
| 3 | T | 20.8 | 49.4 | 370.8 | 274.9 | 0.0 | 0.0 | 0.0 | 0.0 |
| 4 | B | 23.1 | 70.7 | 530.6 | 398.4 | 0.1 | 0.0 | 0.0 | 0.0 |
| 5 | B | 22.4 | 30.5 | 228.9 | 167.7 | 0.0 | 0.0 | 0.0 | 0.0 |
| 6 | T | 21.9 | 61.1 | 458.3 | 342.1 | 0.1 | 0.0 | 0.0 | 0.0 |
| Average | | 22.0 | 60.0 | 450.4 | 337.3 | 0.1 | 0.0 | 0.0 | 0.0 |
| Stdev | | 0.8 | 21.8 | 163.7 | 126.4 | 0.1 | 0.0 | 0.0 | 0.0 |
| Brookstone Silver Bullet | | | | | | | | | |
| Eye | Blade | Velocity (m/s) | Intraocular Pressure (kPa) | Intraocular Pressure (mmHg) | Normalized Energy* ($J/m^2$) | % Injury Risk | | | |
| | | | | | | Hyphema | Lens Damage | Retinal Damage | Globe Rupture |
| 1 | T | 25.4 | 45.4 | 340.2 | 251.5 | 0.0 | 0.0 | 0.0 | 0.0 |
| 2 | B | 21.9 | 83.6 | 626.9 | 474.3 | 0.1 | 0.0 | 0.0 | 0.0 |
| 3 | T | 23.1 | 36.6 | 274.6 | 202.0 | 0.0 | 0.0 | 0.0 | 0.0 |
| 5 | T | 23.9 | 15.23 | 114.3 | 82.9 | 0.0 | 0.0 | 0.0 | 0.0 |
| 6 | T | 22.5 | 64.4 | 483.0 | 361.3 | 0.1 | 0.0 | 0.0 | 0.0 |
| Average | | 23.3 | 49.0 | 367.8 | 274.4 | 0.1 | 0.0 | 0.0 | 0.0 |
| Stdev | | 1.4 | 26.2 | 196.3 | 150.0 | 0.1 | 0.0 | 0.0 | 0.0 |
| Playmaker Toys Flying Saucer | | | | | | | | | |
| Eye | Blade | Velocity (m/s) | Intraocular Pressure (kPa) | Intraocular Pressure (mmHg) | Normalized Energy* ($J/m^2$) | % Injury Risk | | | |
| | | | | | | Hyphema | Lens Damage | Retinal Damage | Globe Rupture |
| 1 | B | 21.8 | 37.9 | 284.3 | 209.3 | 0.0 | 0.0 | 0.0 | 0.0 |
| 2 | B | 19.7 | 49.2 | 369.1 | 273.5 | 0.0 | 0.0 | 0.0 | 0.0 |
| 3 | B | 20.0 | 34.0 | 255.3 | 187.5 | 0.0 | 0.0 | 0.0 | 0.0 |
| 4 | B | 20.3 | 23.3 | 174.8 | 127.5 | 0.0 | 0.0 | 0.0 | 0.0 |
| 5 | B | 16.0 | 29.7 | 223.1 | 163.4 | 0.0 | 0.0 | 0.0 | 0.0 |
| Average | | 19.5 | 34.8 | 261.3 | 192.2 | 0.0 | 0.0 | 0.0 | 0.0 |
| Stdev | | 2.2 | 9.7 | 72.7 | 54.6 | 0.0 | 0.0 | 0.0 | 0.0 |

*Calculated from intraocular pressure.

**Table 9. Velocity, intraocular pressure, correlated normalized energy, and injury risk for fixed wing RC toy helicopters tested. 'T' indicates the top blade impact; "B" indicates the bottom blade impact.**

| Air Hogs Sharpshooter | | | | | | | | | |
|---|---|---|---|---|---|---|---|---|---|
| Eye | Blade | Velocity (m/s) | Intraocular Pressure (kPa) | Intraocular Pressure (mmHg) | Normalized Energy* ($J/m^2$) | % Injury Risk | | | |
| | | | | | | Hyphema | Lens Damage | Retinal Damage | Globe Rupture |
| 1 | T | 19.1 | 39.3 | 294.7 | 217.1 | 0.0 | 0.0 | 0.0 | 0.0 |
| 3 | T | 18.8 | 95.7 | 718.0 | 547.2 | 0.2 | 0.0 | 0.0 | 0.0 |
| 4 | T | 18.4 | 51.1 | 383.6 | 284.7 | 0.1 | 0.0 | 0.0 | 0.0 |
| 5 | T | 18.6 | 19.4 | 145.6 | 106.0 | 0.0 | 0.0 | 0.0 | 0.0 |
| 6 | T | 19.5 | 60.7 | 455.5 | 340.0 | 0.1 | 0.0 | 0.0 | 0.0 |
| Average | | 18.9 | 53.3 | 399.5 | 299.0 | 0.1 | 0.0 | 0.0 | 0.0 |
| Stdev | | 0.4 | 28.3 | 212.3 | 163.9 | 0.1 | 0.0 | 0.0 | 0.0 |
| BanDai Batman | | | | | | | | | |
| Eye | Blade | Velocity (m/s) | Intraocular Pressure (kPa) | Intraocular Pressure (mmHg) | Normalized Energy* ($J/m^2$) | % Injury Risk | | | |
| | | | | | | Hyphema | Lens Damage | Retinal Damage | Globe Rupture |
| 1 | T | 19.7 | 66.0 | 494.7 | 370.4 | 0.1 | 0.0 | 0.0 | 0.0 |
| 2 | B | 19.0 | 94.6 | 709.7 | 540.5 | 0.2 | 0.0 | 0.0 | 0.0 |
| 3 | T | 18.7 | 99.3 | 744.7 | 568.7 | 0.2 | 0.0 | 0.0 | 0.0 |
| 4 | B | 20.0 | 76.1 | 570.7 | 429.8 | 0.1 | 0.0 | 0.0 | 0.0 |
| 6 | T | 17.7 | 66.7 | 500.2 | 374.7 | 0.1 | 0.0 | 0.0 | 0.0 |
| Average | | 19.0 | 80.5 | 604.0 | 456.8 | 0.1 | 0.0 | 0.0 | 0.0 |
| Stdev | | 0.9 | 15.6 | 117.0 | 92.8 | 0.1 | 0.0 | 0.0 | 0.0 |

*Calculated from intraocular pressure.

## Discussion

This is the first study to quantify injury risk for corneal abrasion, hyphema, lens damage, retinal damage, and globe rupture from RC toy helicopter blade impacts. Moreover, this study relates intraocular pressure to eye injury risk for five commercially available RC toy helicopters with various blade designs. Blade design parameters analyzed (mass, length, velocity, and dichotomies of free vs. fixed wing and top vs. bottom blade impacts) did not affect the risk of eye injury associated with eye impact. Despite large differences in design, no single RC toy helicopter blade resulted in higher eye injury risk than the others. Data indicate that the risk of severe eye injury from the tested RC toy helicopter blades is low. However, it is possible that the elevated intraocular pressures measured may indicate delayed onset of eye complications such as glaucoma and cataracts [31, 33]. These underlying complications may go unnoticed and untreated until they have progressed severely [31]. Therefore, eye protection is recommended when operating RC toy helicopters to minimize the risk of eye injury.

Due to the high-speed rotation of the blades, multiple impacts were observed for each eye test. As such, each eye was subjected to a range of impacts from skimming the surface of the eye to momentarily stopping blade rotation. Increased intraocular pressure is correlated to an increased risk of eye injuries [47]. Therefore, the peak intraocular pressure measured in this study corresponds with the impact that would likely be most injurious.

One extreme case of eye injury from a RC helicopter occurred when a blade detached from the shaft and ruptured the eye, resulting in blindness. In this case, the injured person had been inspecting blade alignment of a self-assembled RC helicopter at eye level [52]. While classified as a toy, the RC helicopter that caused this injury was designed for the adult hobbyist and due to its self-assembled nature had not been inspected by the manufacturer prior to testing. Additionally, this injury involved the detachment of the blade from the shaft, a condition not considered as an injury mechanism in the current study due to the pre-assembled nature of the RC toy helicopters tested. This incident illustrates a devastating result of failing to use proper eye protection while testing and flying RC toy helicopters and further supports that eye protection is recommended for children as well as adults when operating RC toy helicopters.

**Conclusions**

The correlations between intraocular pressure and energy presented in this study have potential use in future applications including computational models of the human eye and instrumented synthetic eyes for an advanced anthropomorphic head that measure intraocular pressure during impacts [50]. For impact situations where normalized energy of the striking object is unavailable or incalculable, this study illustrates the use of intraocular pressure for the determination of eye injury risk. Results from this study may provide insight to chronic eye disease as well as foundation data for the design and safe use of RC toy helicopters.

# Chapter 5:
# Eye Injuries from Fireworks are Caused by Projectiles and Not Blast Overpressure


**Abstract**

**Context:** Fireworks cause approximately 2141 eye injuries annually. Currently, it is unknown if the primary injury mechanism is due to blast overpressure or projectile impacts. Although it is suggested that blast overpressure can cause severe eye injuries, there is no clear evidence in the literature to support this. Conversely, projectile impacts have been shown to cause severe eye injuries.

**Objective:** To quantify the response of the human eye subjected to a standard explosive similar to consumer fireworks to determine if blast overpressure alone can cause serious eye injuries.

**Design, Setting, and Participants:** Eighteen free-field explosions of 10 gram charges were conducted at a distance of 22cm, 12cm, and 7cm from the cornea of six isolated postmortem human eyes. The 10 gram charges were used to simulate consumer fireworks in a controlled, repeatable manner. Additionally, five commercially available fireworks (two bottle rockets, three firecrackers) were tested with the same conditions, without an eye present, for comparison.

**Main Outcome Measures:** Total and static overpressures were measured outside the eye using sensors mounted perpendicular and parallel to the explosion, respectively. Intraocular pressure (IOP) was measured with a miniature pressure sensor inserted through the optic nerve. High speed video was recorded for each event. Eyes were examined for injury after each test. IOP was correlated to injury risk using published risk functions based on IOP.

**Results:** No globe ruptures or corneal lacerations were observed. However, video confirmed minor corneal abrasions were caused by projected material. Peak IOP (28.4 ± 9.5 kPa) was linearly correlated to peak total overpressure (33.2 ± 14.1 kPa) for the charges ($R^2$=0.5). All pressures increased with increasing proximity to the cornea. For all tests, injury risk was ≤ 0.01% for hyphema, lens damage, retinal damage, and globe rupture.

**Conclusions:** Blast overpressure from fireworks does not cause severe eye injuries. However, projectiles from fireworks can cause eye injuries. This explains why states with laws restricting firework projectiles observe fewer fireworks-related eye injuries.



**Keywords:** Blast overpressure, Fireworks, Eye injury, Intraocular pressure, Corneal abrasion

## Introduction

Each year, approximately two million people in the United States suffer eye injuries that require treatment [1]. Visual impairment from eye trauma requires costly medical treatment and drastically affects quality of life [18, 53, 54]. The United States Eye Injury Registry (USEIR) estimates that 500,000 years of eyesight are lost annually [17]. Additionally, the economic burden for adult visual disorders is nearly $50 billion a year [19]. Based on data collected between December 31, 1991 and December 31, 2010, the U.S. Consumer Product Safety Commission (CPSC) estimated that approximately 9855 persons are treated in an emergency department for fireworks-related injuries annually, and that 2141 of these are specifically related to the eye [55]. Firework-related injuries in the United States, especially in the month surrounding the Fourth of July, are prevalent among children and adolescents [56, 57, 58]. The eye remains the most frequently injured body part in these incidents, accounting for nearly a quarter of all reported firework-related injuries [56]. Bottle rockets and firecrackers comprise nearly 50% of these injuries [56]. Despite national laws that restrict the size of consumer fireworks, individual state laws are inconsistent with regard to firework purchase and use [59].

Firework explosions produce a sharp increase in ambient pressure (blast overpressure) and temperature followed by an expulsion of material. Misuse of igniting and viewing fireworks poses unique injury risks to the user and bystanders. Much of the current firework-related literature assesses the injurious effects of projected materials to the eye [56, 60, 61]. The effect of projected material is not inconsequential; previous research calculated 100% injury risk for several eye injuries from blunt projectiles [13, 20, 21, 22]. Although some studies state that ocular injuries such as globe rupture and conjunctival hemorrhage can be caused by blast overpressure, there is no clear evidence that directly supports this [62, 63, 64]. The critical question is whether blast overpressure from fireworks can cause ocular injury or if injuries are caused solely by projected material. Previous studies have measured intraocular pressure (IOP) and correlated IOP to eye injury risk [47]. Therefore, the purpose of this research is to measure IOP of enucleated cadaveric eyes during explosions similar to consumer fireworks and assess ocular injuries sustained in order to more fully understand the effect of blast overpressure on the eye.

## Methods

*Design and Setting*

Six human eyes were procured from the North Carolina Eye Bank (Winston Salem, NC, USA) and stored in refrigerated saline. The time interval between death and testing did not exceed 55 days, which was previously shown to not affect tissue response to rupture pressures [4]. As tissue was never exposed to a freeze-thaw cycle, globe integrity was preserved. A miniature pressure sensor (Model 060S, 689 kPa, Precision Measurement Company, Ann Arbor, MI, USA) and a small tube were inserted through the optic nerve into the vitreous fluid and secured in place. This pressure sensor had a frequency response of 10 kHz. A 25 gauge needle was inserted in the small tube and attached to lactated ringer's solution to provide normal human physiologic IOP of 1.993 kPa (14.95 mmHg) throughout the test [47, 23, 65]. Eyes were examined for injury before and after each test to ensure globe integrity was maintained. A fluorescein dye was used to visualize any corneal abrasions. As testing occurred in the open air, eyes were periodically rinsed with saline to maintain tissue hydration.

Open field blast tests were performed on human eyes using a custom test setup designed to measure IOP and blast overpressure. The test setup consisted of a metal frame that suspended the eye approximately 1 m from the ground. A total of four pressure sensors (Model 113B21, 1379 kPa, PCB Piezotronics, Depew, NY, USA) were mounted around the eye (Figure 10). These pressure sensors had a resonance frequency response greater than 500 kHz and measured frequency content up to 100 kHz without distortion. They were designated as "total" or "static" sensors based on their orientation [66]. Total (face-on) sensors measured both the dynamic and static components of the blast overpressure wave, and were mounted perpendicular to the direction of blast wave propagation. Static (side-on) sensors measured the static component of the blast overpressure wave, and were mounted parallel to the direction of wave propagation.

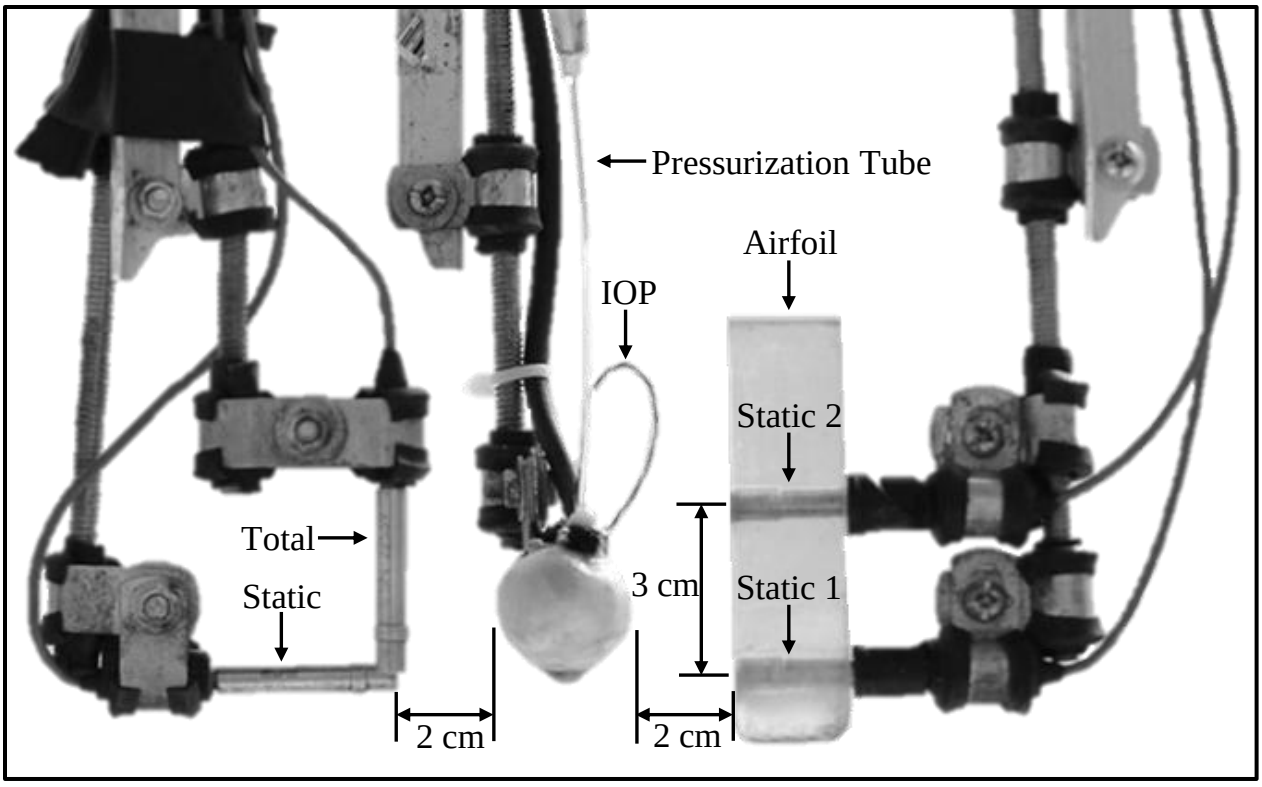


**Figure 10.** Close-up View of Cadaveric Eye Test Setup.

The sensor array consisted of a total overpressure sensor (total) and a static overpressure sensor (static left) adjacent to the eye, and two static overpressure sensors (static right 1, static right 2) mounted 3.0 cm apart in a polycarbonate airfoil-shaped block. The temporal difference between peak overpressures measured by the two static overpressure sensors mounted in the airfoil-shaped block was used to determine the blast overpressure wave velocity.

Due to the large variability of consumer fireworks, this study implemented 10 gram charges fabricated to simulate consumer fireworks in a controlled, repeatable manner. These charges consisted of cardboard tubes filled with 10 grams of Pyrodex® gunpowder that exploded perpendicular to the long axis of the tube. The 10 gram charges were fixed to a metal rod such that the center of the gunpowder was 22 cm, 12 cm, or 7 cm below the cornea. The rod was attached below the center of the gunpowder and did not obstruct the explosion. The long axis of the 10 gram charges was oriented parallel to the anterior-posterior axis of the eye. These three distances were chosen to examine the effect distance has on peak overpressure. The test matrix was designed so tests were conducted with decreasing distance from the cornea. The charge was

offset 2.0 cm from the front of the cornea to minimize the amount of material projected towards the eye.

Five commercially available fireworks (two bottle rockets, three firecrackers) were oriented and tested with the same conditions as the 10 gram charges, but without an eye, for comparison. The high incidence of injuries from firecrackers and aerial devices motivated the testing of firecrackers and bottle rockets in the current study [67, 68].

*Main Outcome Measures*

A data acquisition system (TDAS PRO, Diversified Technical Systems, Inc., Seal beach, CA, USA) collected data at 301887.0 Hz. The standard TDAS PRO anti-aliasing filter (4,300 Hz) was bypassed for this test series because the frequency content of the blast overpressure exceeded 4,300 Hz. However, the TDAS PRO sensor input modules (SIMs) have a bandwidth of 0-25 kHz which acts as a low-pass filter with a frequency cutoff of 25 kHz. All pressure data were zeroed immediately prior to the event. A Phantom v9.1 camera (Vision Research, Wayne, NJ, USA) was used to capture high speed video at 20,000 frames per second with a resolution of 256 x 192 pixels.

Normalized energy was determined using the correlation between IOP and normalized energy developed from projectile testing with a large aluminum rod (11.16 mm diameter) conducted by Duma et al. [47]. The current test series was designed to study the effect of blast on an unprotected eye. Therefore, the area of an open eye affected by a blast is the area of the eye not covered by the eyelid, which is most closely related to the projected area of the 11.16 mm diameter rod. The injury risk function developed by Kennedy and Duma that correlates normalized energy to injury risk was used to determine the injury risk for hyphema, lens damage, retinal damage, and globe rupture [22]. Total overpressure was correlated to IOP for the charges. This relationship was used to determine the expected IOP, normalized energy, and injury risk for the commercial firework tests. Rise time was calculated as the time interval between initiation of positive overpressure and the time at peak overpressure. Positive duration was calculated as the time interval between initiation of positive overpressure and the time when overpressure returned to zero. Impulse was calculated using trapezoidal integration of the total pressure trace over the positive duration.

**Results**

A total of 18 charges were exploded at a distance of 22 cm, 12 cm, or 7 cm from six cadaveric eyes (Table 10). The pressure-time histories of total overpressure, static overpressure, and IOP for a test with a charge at the 7 cm standoff distance are shown in Figure 11. These pressure traces show a steep rise to peak overpressure followed by a positive and subsequent negative overpressure phase that is indicative of a Freidlander waveform [63, 64, 66]. Peak IOP (28.4 ± 9.5 kPa) ranged between 11.3 - 46.7 kPa. Peak total overpressure (33.2 ± 14.1 kPa) and peak static overpressure (27.9 ± 11.4 kPa) ranged between 15.0 - 57.0 kPa and 14.5 - 52.3 kPa, respectively. Normalized energy (67.6 ± 22.8 J/m$^2$) ranged between 2.8 – 112.0 J/m$^2$. Peak IOP correlated to 0.0% injury risk for lens damage, retinal damage, and globe rupture, for all tests. Maximum injury risk for hyphema was 0.01%, which only occurred in three of the five 7 cm tests. Peak IOP (y, kPa) was linearly correlated to peak total overpressure (x, kPa) for the charges ($y = 0.46x + 12.97$, $R^2 = 0.5$).

**Table 10.** Data for 10 gram charge explosion postmortem human eye tests.

| Eye | Standoff Distance | Total Pressure | Static Pressure | Intraocular Pressure | | Wave Velocity | Impulse | Rise Time | Positive Duration |
|---|---|---|---|---|---|---|---|---|---|
| | cm | kPa | kPa | kPa | mmHg | m/s | Pa*s | ms | ms |
| 1 | 22 | 15.0 | 15.7 | 11.3 | 84.8 | 377.4 | 2.1 | 0.079 | 0.282 |
| 2 | 22 | 22.7 | 17.2 | 23.4 | 175.8 | 335.4 | 2.2 | 0.023 | 0.268 |
| 3 | 22 | 24.2 | 18.2 | 26.1 | 195.5 | 335.4 | 2.4 | 0.023 | 0.265 |
| 4 | 22 | 18.1 | 14.5 | 17.6 | 131.9 | 411.7 | 1.9 | 0.023 | 0.288 |
| 5 | 22 | 20.5 | 16.3 | 28.5 | 213.6 | 452.8 | 2.6 | 0.033 | 0.328 |
| 6 | 22 | 26.1 | 19.5 | 24.0 | 180.0 | 362.3 | 2.4 | 0.033 | 0.278 |
| Average | | 21.1 | 16.9 | 21.8 | 163.6 | 379.2 | 2.3 | 0.036 | 0.285 |
| Stdev | | 4.1 | 1.8 | 6.3 | 47.2 | 46.0 | 0.3 | 0.022 | 0.023 |
| 1 | 12 | 24.8 | 24.8 | 23.5 | 176.3 | 476.7 | 2.6 | 0.046 | 0.285 |
| 2 | 12 | 26.4 | 25.6 | 21.7 | 162.9 | 431.3 | 2.8 | 0.023 | 0.285 |
| 3 | 12 | 23.6 | 21.1 | 25.9 | 194.4 | 411.7 | 2.9 | 0.026 | 0.291 |
| 4 | 12 | 29.9 | 27.4 | 21.5 | 161.4 | 431.3 | 4.1 | 0.023 | 0.235 |
| 5 | 12 | 31.2 | 28.7 | 41.0 | 307.2 | 431.3 | 3.1 | 0.040 | 0.258 |
| 6 | 12 | 28.6 | 23.4 | 27.0 | 202.2 | 339.8 | 2.9 | 0.076 | 0.205 |
| Average | | 27.4 | 25.2 | 26.8 | 200.7 | 420.3 | 3.0 | 0.039 | 0.260 |
| Stdev | | 3.0 | 2.7 | 7.3 | 54.7 | 44.9 | 0.5 | 0.020 | 0.034 |
| 1 | 7 | 57.0 | 44.3 | 25.9 | 193.9 | 566.0 | 4.4 | 0.036 | 0.182 |
| 2 | 7 | 54.3 | 38.5 | 38.7 | 290.6 | 431.3 | 4.4 | 0.073 | 0.185 |
| 3 | 7 | 39.8 | 43.5 | 27.6 | 207.4 | 503.1 | 3.5 | 0.079 | 0.229 |
| 4 | 7 | 45.7 | 31.2 | 46.7 | 350.6 | 452.8 | 4.7 | 0.050 | 0.262 |
| 5 | 7 | 53.4 | 52.3 | 45.4 | 340.8 | 476.7 | 3.2 | 0.046 | 0.159 |
| 6 | 7 | 56.6 | 39.4 | 34.7 | 260.1 | 362.3 | 3.9 | 0.023 | 0.182 |
| Average | | 51.1 | 41.6 | 36.5 | 273.9 | 465.4 | 4.0 | 0.051 | 0.200 |
| Stdev | | 6.9 | 7.1 | 8.8 | 65.8 | 68.8 | 0.6 | 0.021 | 0.038 |

**Table 11.** Data for firework explosion tests using bottle rockets (BR) and firecrackers (FC).

| | Standoff Distance | Total Pressure | Static Pressure | Intraocular Pressure* | | Wave Velocity | Impulse | Rise Time | Positive Duration |
|---|---|---|---|---|---|---|---|---|---|
| | cm | kPa | kPa | kPa | mmHg | m/s | Pa*s | ms | ms |
| BR 1 | 22 | 16.6 | 13.4 | 20.7 | 155.0 | 362.3 | 0.8 | 0.023 | 0.123 |
| BR 1 | 22 | 16.0 | 12.8 | 20.4 | 152.9 | 377.4 | 0.8 | 0.020 | 0.123 |
| BR 1 | 22 | 16.3 | 13.2 | 20.5 | 153.8 | 362.3 | 0.7 | 0.020 | 0.119 |
| BR 2 | 22 | 14.7 | 11.7 | 19.8 | 148.3 | 348.3 | 0.6 | 0.020 | 0.109 |
| BR 2 | 22 | 14.0 | 11.2 | 19.5 | 145.9 | 348.3 | 0.6 | 0.020 | 0.099 |
| BR 2 | 22 | 14.6 | 11.8 | 19.7 | 148.1 | 348.3 | 0.6 | 0.023 | 0.109 |
| Average | | 15.4 | 12.3 | 20.1 | 150.7 | 357.8 | 0.7 | 0.021 | 0.114 |
| Stdev | | 1.1 | 0.9 | 0.5 | 3.7 | 11.8 | 0.1 | 0.002 | 0.010 |
| FC 1 | 22 | 5.7 | 4.8 | 15.6 | 117.2 | 348.3 | 0.2 | 0.017 | 0.086 |
| FC 1 | 22 | 7.6 | 6.1 | 16.5 | 123.6 | 362.3 | 0.3 | 0.020 | 0.113 |
| FC 1 | 22 | 5.5 | 4.7 | 15.5 | 116.4 | 348.3 | 0.2 | 0.020 | 0.106 |
| FC 2 | 22 | 4.1 | 3.4 | 14.9 | 111.4 | 348.3 | 0.2 | 0.020 | 0.149 |
| FC 2 | 22 | 3.7 | 4.1 | 14.7 | 110.2 | 362.3 | 0.3 | 0.020 | 0.156 |
| FC 2 | 22 | 4.5 | 3.9 | 15.0 | 112.8 | 335.4 | 0.2 | 0.033 | 0.132 |
| FC 3 | 22 | 5.6 | 4.5 | 15.6 | 116.7 | 348.3 | 0.2 | 0.020 | 0.096 |
| FC 3 | 22 | 6.1 | 5.0 | 15.8 | 118.4 | 348.3 | 0.2 | 0.020 | 0.096 |
| FC 3 | 22 | 5.6 | 4.6 | 15.6 | 116.7 | 362.3 | 0.2 | 0.030 | 0.099 |
| Average | | 5.4 | 4.5 | 15.5 | 115.9 | 351.5 | 0.2 | 0.022 | 0.115 |
| Stdev | | 1.2 | 0.8 | 0.5 | 4.0 | 9.1 | 0.0 | 0.005 | 0.025 |
| BR 1 | 12 | 36.0 | 27.8 | 29.7 | 222.4 | 377.4 | 1.3 | 0.020 | 0.093 |
| BR 1 | 12 | 34.4 | 25.3 | 28.9 | 216.9 | 377.4 | 1.2 | 0.020 | 0.089 |
| BR 1 | 12 | 36.3 | 25.6 | 29.8 | 223.4 | 362.3 | 1.2 | 0.020 | 0.089 |
| BR 2 | 12 | 33.2 | 23.4 | 28.3 | 212.6 | 393.8 | 1.1 | 0.023 | 0.086 |
| BR 2 | 12 | 38.7 | 28.3 | 30.9 | 232.0 | 377.4 | 1.3 | 0.023 | 0.089 |
| BR 2 | 12 | 36.1 | 25.6 | 29.7 | 222.6 | 393.8 | 1.2 | 0.023 | 0.089 |
| Average | | 35.8 | 26.0 | 29.6 | 221.7 | 380.3 | 1.2 | 0.022 | 0.089 |
| Stdev | | 1.9 | 1.8 | 0.9 | 6.6 | 12.0 | 0.1 | 0.002 | 0.002 |
| FC 1 | 12 | 13.7 | 10.2 | 19.3 | 145.0 | 377.4 | 0.5 | 0.020 | 0.086 |
| FC 1 | 12 | 10.3 | 7.9 | 17.7 | 133.0 | 393.8 | 0.3 | 0.023 | 0.063 |
| FC 1 | 12 | 10.9 | 9.1 | 18.0 | 135.1 | 393.8 | 0.4 | 0.020 | 0.099 |
| FC 2 | 12 | 4.9 | 3.6 | 15.2 | 114.3 | 377.4 | 0.4 | 0.043 | 0.162 |
| FC 2 | 12 | 6.7 | 6.0 | 16.1 | 120.5 | 393.8 | 0.5 | 0.023 | 0.212 |
| FC 2 | 12 | 6.2 | 5.2 | 15.8 | 118.8 | 362.3 | 0.5 | 0.089 | 0.245 |
| FC 3 | 12 | 15.2 | 12.9 | 20.0 | 150.0 | 377.4 | 0.5 | 0.020 | 0.083 |
| FC 3 | 12 | 15.8 | 11.9 | 20.3 | 152.2 | 393.8 | 0.6 | 0.023 | 0.096 |
| FC 3 | 12 | 12.5 | 9.6 | 18.8 | 140.9 | 362.3 | 0.5 | 0.020 | 0.086 |
| Average | | 10.7 | 8.5 | 17.9 | 134.4 | 381.3 | 0.5 | 0.031 | 0.126 |
| Stdev | | 4.0 | 3.1 | 1.9 | 13.9 | 13.2 | 0.1 | 0.023 | 0.065 |
| BR 1 | 7 | 71.3 | 46.7 | 46.0 | 345.2 | 431.3 | 2.1 | 0.020 | 0.083 |
| BR 1 | 7 | 78.2 | 55.2 | 49.2 | 369.1 | 431.3 | 2.1 | 0.023 | 0.079 |
| BR 1 | 7 | 70.4 | 48.3 | 45.6 | 342.0 | 411.7 | 1.1 | 0.017 | 0.023 |
| BR 2 | 7 | 77.3 | 54.4 | 48.8 | 366.0 | 452.8 | 2.2 | 0.023 | 0.076 |
| BR 2 | 7 | 82.6 | 51.8 | 51.3 | 384.5 | 476.7 | 2.2 | 0.023 | 0.070 |
| BR 2 | 7 | 68.1 | 44.7 | 44.5 | 333.9 | 476.7 | 1.8 | 0.023 | 0.076 |
| Average | | 74.6 | 50.2 | 47.6 | 356.8 | 446.7 | 1.9 | 0.022 | 0.068 |
| Stdev | | 5.6 | 4.3 | 2.6 | 19.4 | 26.6 | 0.4 | 0.003 | 0.022 |
| FC 1 | 7 | 27.1 | 18.8 | 25.5 | 191.5 | 411.7 | 0.8 | 0.020 | 0.063 |
| FC 1 | 7 | 29.4 | 18.6 | 26.6 | 199.6 | 452.8 | 0.8 | 0.020 | 0.073 |
| FC 1 | 7 | 20.8 | 12.6 | 22.6 | 169.4 | 411.7 | 0.6 | 0.023 | 0.076 |
| FC 2 | 7 | 10.3 | 13.0 | 17.8 | 133.2 | 411.7 | 0.6 | 0.023 | 0.149 |
| FC 2 | 7 | 7.9 | 7.4 | 16.6 | 124.6 | 377.4 | 0.4 | 0.086 | 0.189 |
| FC 2 | 7 | 9.2 | 8.3 | 17.2 | 129.1 | 411.7 | 0.5 | 0.050 | 0.176 |
| FC 3 | 7 | 20.0 | 17.5 | 22.2 | 166.8 | 411.7 | 0.7 | 0.023 | 0.086 |
| FC 3 | 7 | 24.5 | 19.4 | 24.3 | 182.6 | 411.7 | 0.8 | 0.023 | 0.073 |
| FC 3 | 7 | 22.4 | 15.7 | 23.4 | 175.2 | 411.7 | 0.6 | 0.020 | 0.089 |
| Average | | 19.1 | 14.6 | 21.8 | 163.6 | 412.4 | 0.7 | 0.032 | 0.108 |
| Stdev | | 8.0 | 4.5 | 3.7 | 27.9 | 18.9 | 0.1 | 0.022 | 0.049 |

*Intraocular pressure calculated using total pressure.

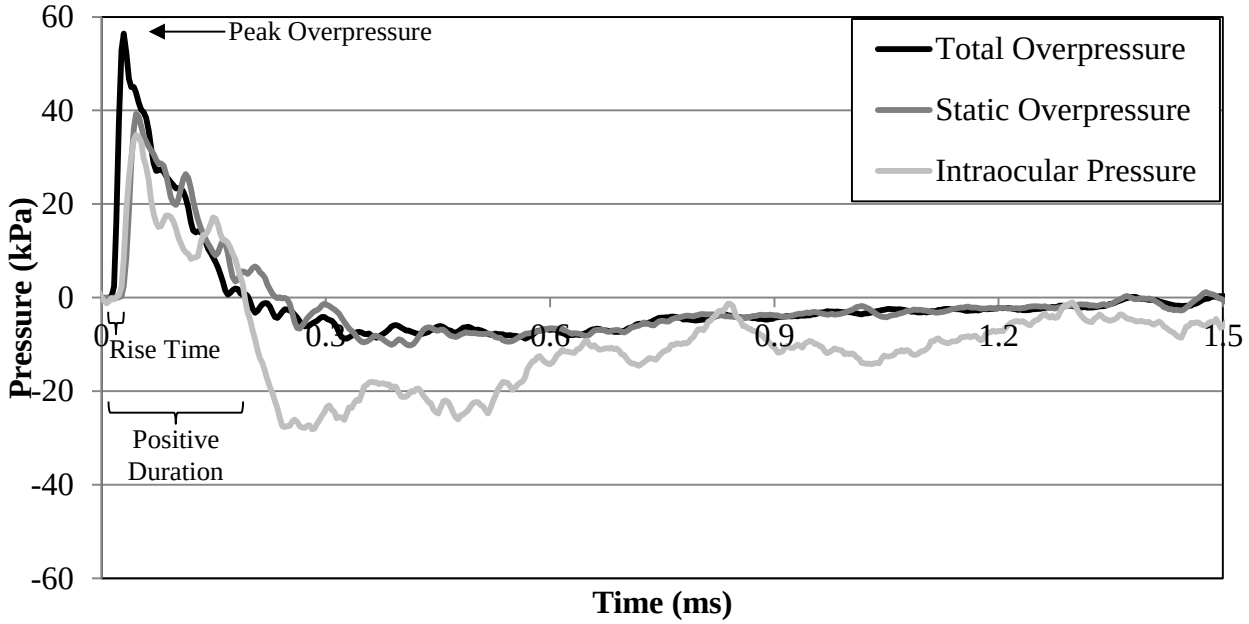


**Figure 11.** Total overpressure, static overpressure, and intraocular pressure due to 10 gram charge explosion at a 7 cm standoff distance from an isolated postmortem human eye. All sensors were zeroed just prior to the event; all pressures are gauge pressures.

A total of 18 commercial bottle rockets and 27 commercial firecrackers were exploded without an eye present (Table 11). For the bottle rockets, peak total overpressure (41.9 ± 25.5 kPa) and peak static overpressure (29.5 ± 16.3 kPa) ranged between (14.0 – 82.6 kPa) and (11.2 – 55.2 kPa), respectively. Normalized energy (77.4 ± 28.5 J/m$^2$) ranged between 46.2 – 123.0 J/m$^2$. Peak IOP correlated to 0.00% injury risk for lens damage, retinal damage, and globe rupture, and maximum injury risk for hyphema was 0.01%, which only occurred at the 7 cm distance for the bottle rocket tests. For the firecrackers, peak total overpressure (11.7 ± 7.6 kPa) and peak static overpressure (9.2 ± 5.2 kPa) ranged between (3.7 – 29.4 kPa) and (3.4 – 19.4 kPa), respectively. Normalized energy (43.7 ± 8.5 J/m$^2$) ranged between 34.9 – 63.4 J/m$^2$. Peak IOP correlated to 0.00% injury risk for hyphema, lens damage, retinal damage, and globe rupture for the firecracker tests.

No globe ruptures or corneal lacerations were observed; however, minor corneal abrasions were observed. The abrasion size and pattern suggested injuries were sustained from unspent Pyrodex® being projected onto the eye during the event, which was confirmed with high speed video (Figure 12). As expected, more abrasions were observed as the standoff distance decreased.

**Figure 12.** (Left) Photograph before 5 cm standoff distance test. (Right) Post-test photograph with arrows indicating corneal abrasions. Fluorescein dye used to better visualize corneal abrasions under a blue light. Bright white dot is a reflection of light.

**Discussion**

This study quantified the response and injury outcome of postmortem human eyes exposed to blast overpressure. Major eye injuries such as globe rupture were not observed. However, minor corneal abrasions were observed to have been caused by projected material. Hyphema, lens damage, retinal damage, and globe rupture were not predicted to have occurred based on the peak overpressures recorded in the current study. The lack of major injuries from firework blast overpressure indicates that firework blast overpressure does not cause serious eye injuries. However, it was shown that eye injuries from fireworks can be caused by projectile impacts.

Previous studies on the epidemiology of fireworks-related injuries presented at emergency departments note that injuries to the eyeball (21%) and face (20%) occur frequently [60]. One study reported firecrackers and bottle rockets accounted for 50% of these eye injuries and noted rockets alone comprised 71% of the studied cases where severe eye injuries resulted in vision loss [56]. Due to their aerial nature, bottle rockets pose a larger threat of projectile injury than do firecrackers that remain on the ground. Results from the current study support the higher risk of eye injuries caused by bottle rockets, as they are projectiles and projectiles have been shown to cause eye injuries.

This study implemented 10 gram charges fabricated to simulate consumer fireworks in a controlled, repeatable manner. It was observed for all tests that as standoff distance increased, rise time remained constant, peak overpressure decreased, positive duration increased, and impulse decreased. Rise time did not vary greatly between the 10 gram charges, bottle rockets and firecrackers. The bottle rockets produced larger peak over pressures than the 10 gram charges while the firecrackers produced smaller peak overpressures than the 10 gram charges. Regardless, the calculated injury risk for all eye injuries assessed was less than or equal to 0.01% for all tests. The 10 gram charges had longer positive durations than the bottle rockets and firecrackers. Longer positive durations are potentially more injurious, as the increased exposure to pressure allows soft biological tissues to experience greater deformations. Impulse was highest for the 10 gram charges, which is not surprising due to the combined higher peak overpressure and longer positive overpressure duration.

Blast overpressure is comprised of a positive pressure phase followed by a negative pressure phase (with respect to atmospheric pressure) that is indicative of a Freidlander waveform [63, 64, 23]. It is of interest to note the IOP trace shows a relatively large negative pressure. However, as all sensors were zeroed just prior to the event, the pressures reported in the current study are gauge pressures and not absolute pressures. Therefore, the eye does not experience a true a negative IOP, but rather a reduction in pressure relative to atmospheric pressure. It has been hypothesized that cavitation of fluids *in vivo,* caused by a decrease in pressure, can result in tissue injury [69]. Cavitation threshold is affected by temperature, surface tension, dissolved gas, impurities, and viscosity [70, 71, 72]. The cavitation threshold for water ranges between gauge pressures of -100 kPa and -140 MPa depending on the water composition and test method [72]. Previous studies modeled cavitation in the brain due to blast overpressure using a cavitation threshold of -100 kPa [70, 73]. As IOP did not fall below –50 kPa in the current study, it was not expected that cavitation was a possible cause of injury. Additionally, it is expected that the gelatinous nature of the vitreous fluid would alter the cavitation threshold compared to that of water.

Federal firework regulations currently limit the amount of pyrotechnic material in consumer fireworks to 50 mg for firecrackers and 130 mg for bottle rockets in order to minimize the risk of injury from these devices [74]. Individual state laws may additionally prohibit the distribution,

purchase, and use of these devices to further decrease injury risk from misuse. Previous studies noted that states and countries banning the use of fireworks observed lower incidences of eye injuries due to fireworks [68, 75]. As of June 1, 2011, only four states completely ban fireworks, including those allowed by CPSC regulations: Delaware, Massachusetts, New Jersey, and New York [59]. Therefore, it is expected that states without fireworks regulations will observe a higher incidence of fireworks-related injuries than states that regulate fireworks. Where fireworks are allowed, it is suggested that persons adhere to rules of their use and be familiar with the risks associated with projected material.

*Limitations*

Postmortem human eyes were exposed to multiple events in the current study. This maximized the use of biological tissue and provided a paired data set, thereby eliminating the confounding effects of subject variability. It is possible that successive events can cause microdamage to the tissue which can result in premature failure during a subsequent test that would not have occurred otherwise. The testing order was designed to minimize this by testing the lowest severity first (22 cm), followed by the medium severity (12 cm), and finally the highest severity (7 cm). Additionally, blast overpressures in the current study were of relatively low severity and did not result in severe injuries. Therefore, the potential for adverse effects of multiple exposures was considered negligible.

All postmortem eye tests were performed with an isolated eye in the current study. Anatomically, the eye is located within the orbit and is surrounded by the soft tissue, musculature, and boney structures of the face. These numerous reflective surfaces create complex pressure waves around the eye during blast overpressure events. Consequently, it is extremely difficult to interpret the isolated response of the eye with these boundary conditions. Since there is currently no data regarding the response of the human eye to blast overpressure, the eye was tested in isolation to minimize the confounding effects of multiple reflective pressure waves. This facilitated the direct quantification of the eye response to blast overpressure. Future studies should be performed to understand the effect multiple reflective pressure waves from these structures.

*Other Applications*

This is the first study to investigate the effects of blast overpressure on the human eye. The blast overpressures recorded in the current study represent low blast energies. For comparison, a 10 gram charge of Pyrodex®, at 22 cm, 12 cm, and 7 cm standoff distances correspond to detonating 0.45 kg TNT at approximately 7.33 m, 4.57 m, and 3.05 m, respectively [66]. Higher severity blast overpressures can be experienced during military combat. Combat-related blast injuries are occurring more frequently with the increased use of explosives and improvised explosive devices (IEDs) in current military conflicts [76]. While the lung was once most susceptible to blast injury, the use of improved protective chest equipment has disproportionally left the face and eyes vulnerable to concomitant blast injuries [76]. Approximately 5% (797) of all reported injuries sustained in the War in Iraq between 2003-2005 were eye injuries [61]. Studies have reported approximately 82% of all severe ocular injuries sustained during military combat are the result of munitions fragmentation [51, 77]. Additionally, as many military explosives are buried, the risk of injury from projectiles would be expected to be much greater. It is unclear whether severe ocular injuries such as lens damage, retinal damage or globe rupture can be caused by higher blast overpressures. However, the relationship between peak IOP and peak total overpressure noted in this study indicates that an extremely large peak blast overpressure would be required to induce an IOP large enough to cause globe rupture, given an internal rupture pressure of 970 ± 290 kPa [47, 23]. It is expected that more lethal corporal injuries resulting from such a large blast event would likely take precedence over potential ocular injuries. Further studies should be performed to evaluate the response and injuries resulting from higher blast overpressures. It should be noted that such a study would require the use of high energy explosives such as TNT, C4, or Comp-B.

**Conclusions**

This study quantifies the risk of eye injuries caused by firework blast overpressure. Serious eye injuries such as globe rupture were neither observed nor predicted by the IOP induced by the blast overpressure. However, minor corneal abrasions were observed after each test. High speed video analysis confirmed that the corneal abrasions were caused by projected unspent gunpowder. The extent of corneal abrasion depended on charge standoff distance. The combined presence of injuries caused by projected material and lack of injuries directly caused by blast overpressure indicates that serious eye injuries from fireworks can be caused by projectiles and not blast overpressure.

# Chapter 6:
# Conclusions

## Research Summary

The research presented in this thesis investigates eye injuries caused by blunt impacts and blast overpressure as part of an ongoing investigation to accurately quantify and predict eye injuries and injury mechanisms for various loading schemes. No serious eye injuries were observed for any of the tests and all tests resulted in low predicted injury risks consistent with the lack of observed injury. This reserach provides a robust low injury level dataset for eye injuries. This data could be useful for designing and validating computational models and anthropomorphic test device eyes, and serves as a basis for future work with more dangerous projectiles and higher pressure levels. Additional data combined with that described in this thesis could be used to design safer eye protection from blunt impact and blast overpressure which could mitigate the frequency of severe eye injuries. The research presented in this thesis represents a portion of a larger investigation of biomedical engineering and injury biomechanics [78-197].

## Publication Outline

The research presented in this thesis has been submitted for publication in various journals and conference proceedings. Table 12 notes the publication destinations for each chapter. All chapters are presented in this thesis in their publication forms with modification of only figure, table, and reference numbers.

**Table 12. Publication Outline**

| Chapter | Title | Journal/*(Conference)* |
|---|---|---|
| 2 | Evaluating the risk of eye injuries: intraocular pressure during high speed projectile impacts | Current Eye Research* *(Biomedical Engineering Society 2011 Annual Meeting)§* |
| 3 | Eye injury risk from water stream impact: biomechanically based design parameters for water toy and park design | Current Eye Research† |
| 4 | Eye injury risk associated with remote control toy helicopter blades | *(Rocky Mountain Bioengineering Symposium)†* |
| 5 | Eye injuries from fireworks are caused by projectiles and not blast overpressure | Journal of the American Medical Association‡ |
| * Published, † Accepted, ‡ Submitted, § Presented | | |

## References


[1] McGwin G Jr, Xie A, Owsley C. Rate of eye injury in the United States. *Arch Ophthalmol*. 2005;123(7):970-976.

[2] Duma SM, Jernigan MV, Stitzel JD, Herring IP, Crowley JS, Brozoski FT, Bass CR. The effect of frontal air bags on eye injury patterns in automobile crashes. *Arch Ophthalmol*. 2002;120(11):1517-1522.

[3] Fukagawa K, Tsubota K, Kimura C, Hata S, Mashita T, Sugimoto T, Oguchi Y. Corneal endothelial cell loss induced by air bags. *Ophthalmology.* 1993;100(12):1819-1823.

[4] Kennedy EA, Voorhies KD, Herring IP, Rath AL, Duma SM. Prediction of severe eye injuries in automobile accidents: Static and dynamic rupture pressure of the eye. *Annu Proc Assoc Adv Automot Med*. 2004;48:165-179.

[5] Kisielewicz LT, Kodama N, Ohno S, Uchio E. Numerical prediction of airbag caused injuries on eyeballs after radial keratotomy. Society of Automotive Engineers International Congress and Exposition, Detroit, MI. Paper number: 980906, 1998.

[6] Duma SM, Crandall JR. Eye injuries from airbags with seamless module covers. *J Trauma*. 2000;48(4):786-789.

[7] Duma SM, Kress TA, Porta DJ, Woods CD, Snider JN, Fuller PM, Simmons RJ. Airbag-induced eye injuries: a report of 25 cases. *J Trauma*. 1996;41(1):114-119.

[8] Duma SM, Rath AL, Jernigan MV, Stitzel JD, Herring IP. The effects of depowered airbags on eye injuries in frontal automobile crashes. *Am J Emerg Med*. 2005;23(1):13-19.

[9] Duma SM, Jernigan MV. The effects of airbags on orbital fracture patterns in frontal automobile crashes. *Ophthal Plast Reconstr Surg*. 2003;19(2):107-111.

[10] Hansen GA, Stitzel JD, Duma SM. Incidence of elderly eye injuries in automobile crashes: the effects of lens stiffness as a function of age. *Annu Proc Assoc Adv Automot Med*. 2003;47:147-163.

[11] Duma SM, Kress TA, Porta DJ, Simmons RJ, Alexander CL, Woods CD. Airbag-induced eye injuries: experiments with in situ cadaver eyes. *Biomed Sci Instrum.* 1997;33:106-111.

[12] Duma SM, Kress TA, Porta DJ, Simmons RJ, Alexander CL. An experimental study of airbag impact to the orbit using an instrumented Hybrid III headform. *Biomed Sci Instrum.* 1997;33:59-64.

[13] Kennedy EA, Ng TP, McNally C, Stitzel JD, Duma SM. Risk functions for human and porcine eye rupture based on projectile characteristics of blunt objects. *Stapp Car Crash J.* 2006;50:651-671.

[14] Vinger PF, Duma SM, Crandall JR. Baseball hardness as a risk factor for eye injuries. *Arch Ophthalmol*. 1999;117(3):354-358.

[15] Kennedy EA, Ng TP, Duma SM. Evaluating eye injury risk of Airsoft pellet guns by parametric risk functions. *Biomed Sci Instrum.* 2006;42:7-12.

[16] Heier JS, Enzenauer RW, Wintermeyer SF, Delaney M, LaPiana FP. Ocular injuries and diseases at a combat support hospital in support of Operations Desert Shield and Desert Storm. *Arch Ophthalmol*. 1993;111(6):795-798.

[17] Eye trauma: epidemiology and prevention. United States Eye Injury Registry Online Web site. http://www.useironline.org/Prevention.htm. Accessed November 7, 2011.

[18] Frick KD, Gower EW, Kempen JH, Wolff JL. Economic impact of visual impairment and blindness in the United States. *Arch Ophthalmol*. 2007;125(4):544-550.

[19] Rein DB, Zhang P, Wirth KE, Lee PP, Hoerger TJ, McCall N, Klein R, Tielsch JM, Vijan S, Saaddine J. The economic burden of major adult visual disorders in the United States. *Arch Ophthalmol*. 2006;124(12):1754-1760.

[20] Duma SM, Ng TP, Kennedy EA, Stitzel JD, Herring IP, Kuhn F. Determination of significant parameters for eye injury risk from projectiles. *J Trauma*. 2005;59(4):960-964.

[21] Kennedy EA, Inzana JA, McNally C, Duma SM, Depinet PJ, Sullenberger KH, Morgan CR, Brozoski FT. Development and validation of a synthetic eye and orbit for estimating the potential for globe rupture due to specific impact conditions. *Stapp Car Crash J*. 2007;51:381-400.

[22] Kennedy EA, Duma SM. Eye injury risk functions for human and FOCUS eyes: hyphema, lens dislocation, and retinal damage. Prepared for: US Army Medical Research and Materiel Command, Fort Detrick, MD. Updated July 8, 2011.

[23] Bisplinghoff JA, McNally C, Duma SM. High-rate internal pressurization of human eyes to predict globe rupture. *Arch Ophthalmol*. 2009;127(4):520-523.

[24] Bisplinghoff JA, McNally C, Manoogian SJ, Duma SM. Dynamic material properties of the human sclera. *J Biomech*. 2009;42(10):1493-1497.

[25] Bisplinghoff JA, McNally C, Yang S, Herring IP, Brozoski FT, Duma SM. High rate internal pressurization of the human eye to determine dynamic rupture pressure. *Biomed Sci Instrum.* 2008;44:117-122.

[26] Bisplinghoff JA, McNally C, Brozoski FT, Duma SM. Dynamic material property measurements of human eyes. *Biomed Sci Instrum.* 2008; 44:177-182.

[27]. Magnante DO, Bullock JD, Green WR. Ocular explosion after peribulbar anesthesia: case report and experimental study. *Ophthalmology*. 1997;104(4):608-615.

[28] Bullock JD, Warwar RE, Green WR. Ocular explosion during cataract surgery: a clinical, histopathological, experimental, and biophysical study. *Trans Am Ophthalmol Soc*. 1998;96:243-81.

[29] Bullock JD, Warwar RE, Green WR. Ocular explosions from periocular anesthetic injections: a clinical, histopathological, experimental, and biophysical study. *Ophthalmology*. 1999;106(12):2341-2353.

[30] Stitzel JD, Hansen GA, Herring IP, Duma SM. Blunt trauma of the aging eye: injury mechanisms and increasing lens stiffness. *Arch Ophthalmol*. 2005;123(6):789-794.

[31] Sihota R, Kumar S, Gupta V, Dada T, Kashyap S, Insan R, Srinivasan G. Early predictors of traumatic glaucoma after closed globe injury: trabecular pigmentation, widened angle recess, and higher baseline intraocular pressure. *Arch Ophthalmol*. 2008;126(7):921-926.

[32] Rumelt S, Rehany U. The influence of surgery and intraocular lens implantation timing on visual outcome in traumatic cataract. *Graefes Arch Clin Exp Ophthalmol*. 2010;248(9):1293-1297.

[33] Sihota R, Sood NN, Agarwal HC. Traumatic glaucoma. *Acta Ophthalmol Scand*. 1995;73(3):252-254.

[34] Dannenberg AL, Parver LM, Brechner RJ, Khoo L. Penetration eye injuries in the workplace. The National Eye Trauma System Registry. *Arch Ophthalmol*. 1992;110(6):843-8.

[35] Pieramici DJ, Sternberg P Jr, Aaberg, TM Sr, Bridges WZ Jr, Capone A Jr, Cardillo JA, de Juan E Jr, Kuhn F, Meredith TA, Mieler WF, Olsen TW, Rubsamen P, Stout T. A system for classifying mechanical injuries of the eye (globe). The Ocular Trauma Classification Group. *Am J Ophthalmol*. 1997;123(6):820-831.

[36] Kennedy EA, Duma SM. The effects of the extraocular muscles on eye impact force-deflection and globe rupture response. *J Biomech*. 2008;41(16):3297-3302.

[37] Kennedy EA, McNally C, Duma SM. Experimental techniques for measuring the biomechanical response of the eye during impact. *Biomed Sci Instrum.* 2007;43:7-12.

[38] Kennedy EA, Bonivtch AR, Manoogian SJ, Stitzel JD, Herring IP, Duma SM. The effects of extraocular muscles on static displacements of the human eye. *Biomed Sci Instrum*. 2006;42:372-377.

[39] Clark SA, Thiel EL, Kennedy EA. An intraocular pressure measurement technique for eye impact testing – biomed 2010. *Biomed Sci Instrum*. 2010;46:434-439.

[40] Bisplinghoff JA, Duma SM. Evaluation of eye injury risk from projectile shooting toys using the focus headform – biomed 2009. *Biomed Sci Instrum*. 2009;45:107-112.

[41] Kennedy EA, Stitzel JD, Duma SM. Matched experimental and computational simulations of paintball eye impacts. *Biomed Sci Instrum.* 2008;44:243-248.

[42] Power ED, Duma SM, Stitzel JD, Herring IP, West RL, Bass CR, Crowley JS, Brozoski FT. Computer modeling of airbag-induced ocular injury in pilots wearing night vision goggles. *Aviat Space Environ Med*. 2002;73(10):1000-1006.

[43] Stitzel JD, Duma SM, Cormier JM, Herring IP. A nonlinear finite element model of the eye with experimental validation for the prediction of globe rupture. *Stapp Car Crash J*. 2002;46:81-102.

[44] Weaver AA, Loftis KL, Tan JC, Duma SM, Stitzel JD. CT based three-dimensional measurement of orbit and eye anthropometry. *Invest Ophthalmol Vis Sci*. 2010;51(10):4892-4897.

[45] Deng Z, Guensch, GR, McKinstry CA, Mueller RP, Dauble DD, Richmond MC. Evaluation of Fish-Injury Mechanisms during Exposure to Turbulent Shear Flow. *Can J Fish Aquat Sci*. 2005;62(7):1513-1522.

[46] Nietzel DA, Richmond MC, Dauble DD, Mueller RP. Laboratory Studies on the Effects of Shear on Fish. Prepared for the U.S. Department of Energy, Idaho Operations Office. 2000.

[47] Duma SM, Bisplinghoff JA, Senge DM, McNally C, Alphonse VD. Evaluating the risk of eye injuries: Intraocular pressure during high speed projectile impacts. *Curr Eye Res*. 2012;37(1):43-49.

[48] Fatality Assessment and Control Evaluation (FACE) Program. Ranch worker killed by pressurized water striking eye. Case Report: 06-OR-025. 2006.

[49] DeAngelis DD, Oestreicher JH. Traumatic enucleation from a high-pressure water jet. *Arch Ophthalmol*. 1999;117(1):127-128.

[50] Weaver AA, Loftis KL, Duma SM, Stitzel JD. Biomechanical modeling of eye trauma for different orbit anthropometries. *J Biomech*. 2011;44(7):1296-1303.

[51] Thach AB, Johnson AJ, Carroll RB, Huchun A, Ainbinder DJ, Stutzman RD, Blaydon SM, Demartelaere SL, Mader TH, Slade CS, George RK, Ritchey JP, Barnes SD, Fannin LA. Severe eye injuries in the war in Iraq, 2003-2005. *Ophthalmology*. 2008;115(2): 377-382.

[52] Lee VY, Liu DT, Leung GY, Luo Y, Lam PT. Devastating projectile injury of the eye caused by a remote-controlled toy helicopter. Hong Kong Med J. 2009;15(6):492-493.

[53] Vitale S, Cotch MF, Sperduto RD. Prevalence of visual impairment in the United States. *JAMA*. 2011;295(18):2158-2163.

[54] Kuhn F, Morris R, Witherspoon CD, Mann L. Epidemiology of blinding trauma in the United States Eye Injury Registry. *Ophthalmic Epidemiol*. 2006;13(3):209-216.

[55] US Consumer Product Safety Commission. National Electronic Injury Surveillance System data, 1991-2010. [Machine-readable public use data type.] Washington, DC: US Consumer Product Safety Commission, 2012.

[56] Smith GA, Knapp JF, Barnett TM, Shields BJ. The rocket's red glare, the bombs bursting in air: fireworks-related injuries to children. *Pediatrics*. 1996;98(1):1-9.

[57] From the Centers for Disease Control and Prevention Brief Report: Injuries Associated with Homemade Fireworks – Selected States, 1993-2004. *JAMA*. 2004;292(13):1545-1546.

[58] [No authors listed]. From the Centers for Disease Control and Prevention. Injuries from fireworks in the United States. *JAMA*. 2000;284(3):302.

[59] Fireworks, Publication #12. US Consumer Product Safety Commission. http://www.cpsc.gov/cpscpub/pubs/012.html. Accessed December 16, 2011.

[60] Witsaman RJ, Comstock RD, Smith GA. Pediatric fireworks-related injuries in the United States: 1990-2003. *Pediatrics*. 2006;118(1):296-303.

[61] Khan M, Reichstein D, M Recchia F. Ocular consequences of bottle rocket injuries in children and adolescents. *Arch Ophthalmol*. 2011;129(5):639-642.

[62] DePalma RG, Burris DG, Champion HR, Hodgson MJ. Blast Injuries. *N Engl J Med*. 2005;352(13):1335-1342.

[63] Ritenour AE, Baskin TW. Primary blast injury: Update on diagnosis and treatment. *Crit Care Med*. 2008;36(7 Suppl): S311-S317.

[64] Mayorga MA. The Pathology of primary blast overpressure injury. *Toxicology*. 1997;121(1):17-28.

[65] Sponsel WE, Gray W, Scribbick FW, Stern AR, Weiss CE, Groth SL, Walker JD. Blunt eye trauma: Empirical histopathologic paintball impact thresholds in fresh mounted porcine eyes. *Invest Ophthalmol Vis Sci*. 2011;52(8):5157-5166.

[66] Stuhmiller JH, Phillips III YY, Richmond DR. The physics and mechanisms of primary blast injury. In: Bellamy RF, Zajtchuk R, eds. *Conventional Warfare: Ballistic, Blast and Burn Injuries.* Washington, DC: Office of the Surgeon General at TMM Publications; 1990:241-270. http://bordeninstitute.army.mil/published.html. Accessed July 19, 2011.

[67] McFarland LV, Harris JR, Kobayashi JM, Dicker RC. Risk factors for fireworks-related injury in Washington State. *JAMA*. 1984;251(24):3251-3254.

[68] Kuhn F, Morris RC, Witherspoon DC, Mann L, Mester V, Módis L, Berta A, Bearden W. Serious fireworks-related eye injuries. *Ophthalmic Epidemiol*. 2000;7(2):139-148.

[69] Nakagawa A, Manley GT, Gean AD, Ohtani K, Armonda R, Tsukamoto A, Yamamoto H, Takayama K, Tominaga T. Mechanisms of primary blast-induced traumatic brain injury: insights from shock-wave research. *J Neurotrauma.* 2011;28(6):1101-1119.

[70] Panzer MB, Myers BS, Capehart BP, Bass CR. Development of a finite element model for blast brain injury and the effects of CSF cavitation. *Ann Biomed Engr*. In press.

[71] Webb IR, Payne SJ, Coussios CC. The effect of temperature and viscoelasticity on cavitation dynamics during ultrasonic ablation. *J Acoust Soc Am.* 2011;130(5):3458-3466.

[72] Herbert E, Balibar S, Caupin F. Cavitation pressure in water. *Phys Rev E.* 2006;74:041603.

[73] Moss WC, King MJ, Blackman EG. Skull flexure from blast waves: a mechanism for brain injury with implications for helmet design. *Phys Rev Lett*. 2009;103(10):108702.

[74] [No authors listed]. US Consumer Product Safety Commission Office of Compliance Summary of Fireworks Regulations, 16. C.F.R. Part 15 & 1507. Consumer Product Safety Commission Web site. http://www.cpsc.gov/businfo/regsumfirework.pdf. Published: January, 2001. Accessed: December 16, 2011.

[75] Wilson RS. Ocular fireworks injuries and blindness. An analysis of 154 cases and a three-state survey comparing the effectiveness of model law regulation. *Ophthalmology*. 1982;89(4):291-297.

[76] Thomas R, McManus JG, Johnson A, Mayer P, Wade C, Holcomb JB. Ocular injury reduction from ocular protection use in current combat operations. *J Trauma*. 2009;66(4 Suppl): S99-S103.

[77] Mader TH, Carroll RD, Slade CS, George RK, Ritchey JP, Neville SP. Ocular war injuries of the Iraqi Insurgency, January-September 2004. *Ophthalmology*. 2006;113(1):97-104.

[78] Bass CR, Duma SM, Crandall JR, George S, Kuppa S, Khaewpong N, Sun E, Eppinger R. The interaction of air bags with upper extremity test devices. Proceedings of the Institution of Mechanical Engineers Part D - Journal of Automobile Engineering. 216(D10):795-803, 2002.

[79] Bass CR, Duma SM, Crandall JR, Pilkey WD, Khaewpong N, Eppinger RH. "The Interaction of Airbags with Cadaveric Upper Extremities," Proceedings of the 41st International Stapp Car Crash Conference, Orlando, Florida, November, 1997.

[80] Beeman SM, Kemper AR, Madigan ML, Duma SM. Effects of bracing on human kinematics in low-speed frontal sled tests. *Ann Biomed Eng*. 2011;39(12):2998-3010.

[81] Beeman SM, Kemper AR, Madigan ML, Franck CT, Loftus SC. Occupant kinematics in low-speed frontal sled tests: Human volunteers, Hybrid III ATD, and PMHS. *Accid Anal Prev*. 2012;47:128-139.

[82] Beyer JA, Rowson S, Duma SM. Concussions experienced by Major League Baseball catchers and umpires: field data and experimental baseball impacts. *Ann Biomed Eng*. 2012;40(1): 150-159.

[83] Bisplinghoff JA, Duma SM. The effect of stress and strain formulations on the representation of biological tissue mechanical properties – biomed 2009. *Biomed Sci Instrum.* 2009;45:389-394.

[84] Bolin D, Kemper A, Brolinson PG. Current concepts in the evaluation and management of stress fractures. *Curr Sports Med Rep*. 2005;4(6): 295-300.

[85] Brolinson PG, Manoogian S, McNeely D, Goforth M, Greenwald R, Duma S. Analysis of linear head accelerations from collegiate football impacts. Curr Sports Med Rep. 2006;5(1):23-28.

[86] Bussone WR, Duma SM. The effect of gender and body size on angular accelerations of the head observed during everyday activities – biomed 2009. *Biomed Sci Instrum*. 2010;46:166-171.

[87] Cormier J, Manoogian S, Bisplinghoff J, Rowson S, Santago A, McNally C, Duma SM, Bolte J. Biomechanical response of the human face and corresponding biofidelity of the FOCUS headform. International Journal of Passenger Cars - Mechanical Systems. 3(1):842-859, 2010.

[88] Cormier J, Manoogian S, Bisplinghoff J, Rowson S, Santago A, McNally C, Duma S, Bolte J 4th. The tolerance of the frontal bone to blunt impact. *J Biomech Eng.* 2011;133(2):021004.

[89] Cormier J, Manoogian S, Bisplinghoff J, Rowson S, Santago A, McNally C, Duma S, Bolte J 4th. The tolerance of the maxilla to blunt impact. *J Biomech Eng*. 2011;133(6):064501.

[90] Cormier J, Manoogian S, Bisplinghoff J, Rowson S, Santago A, McNally C, Duma S, Bolte Iv J. The tolerance of the nasal bone to blunt impact. *Ann Ad Automot Med*. 2010;54:3-14.

[91] Cormier J, Duma S. Epidemiology of facial Fractures in automotive collisions. *Ann Adv Automot Med.* 2009;53:169-176.

[92] Cormier J, Manoogian S, Bisplinghoff J, McNally C, Duma S. The use of acoustic emission in facial fracture detection. *Biomed Sci Instrum*. 2008;44:147-152.

[93] Cormier JM, Manoogian SJ, Bisplinghoff JA, Rowson S, Santago AC, McNally C, Duma SM, Bolte JH. Biomechanical Response of the Human Face and Corresponding Biofidelity of the FOCUS Headform. Journal of Passenger Cars - Mechanical Systems. 119(6): 2010-01-1317, 2010.

[94] Cormier JM, Stitzel JD, Duma SM, Matsuoka F. Regional variation is the structural response and geometrical properties of human ribs. *Annu Proc Assoc Automot Med.* 2005;49:153-170.

[95] Cormier JM, Stitzel JD, Hurst WJ, Porta DJ, Jones J, Duma SM. Predicting zygoma fractures from baseball impact. *Biomed Sci Instrum*. 2006;42:142-147.

[96] Crisco JJ, Wilcox BJ, Beckwith JG, Chu JJ, Duhaime AC, Rowson S, Duma SM, Maerlender AC, McAllister TW, Greenwald RM. Head impact exposure in collegiate football players. *J Biomech*. 2011;44(15):2673-2678.

[97] Crisco JJ, Fiore R, Beckwith JG, Chu JJ, Brolinson PG, Duma S, McAllister TW, Duhaime AC, Greenwald RM. Frequency and location of head impact exposures in individual collegiate football players. *J Athl Train*. 2010;45(6):549-559.

[98] Crowley JS, Brozoski FT, Duma SM, Kennedy EA. Development of the Facial and Ocular Countermeasures Safety (FOCUS) headform. *Aviat Space Environ Med*. 2009;80(9):831.

[99] Daly M, Duma SM, Stitzel JD. Retrospective identification of subject anthropometry using computed tomography of the leg. *Biomed Sci Instrum*. 2006;42:114-119.

[100] Daniel RW, Rowson S, Duma SM. Head Impact Exposure in Youth Football. *Ann Biomed Eng*. 2012;40(4):976-981.

[101] Duma SM, Rowson, S. Every Newton Hertz: A macro to micro approach to investigating brain injury. *Conf Proc IEEE Eng Med Biol Soc*. 2009;1123-1126.

[102] Duma SM, Bass CR, Klopp GS, Grillo N, Micek TJ, Crandall JR, Pilkey WD. A technique for using strain gauges to evaluate airbag interaction with cadaveric upper extremities. *Biomed Sci Instrum*. 2007;33:47-52.

[103] Duma SM, Boggess BM, Crandall JR, MacMahon CB. Injury risk function for the small female wrist in axial loading. *Accid Anal Prev*. 2003;35(6):869-875.

[104] Duma SM, Boggess BM, Crandall JR, MacMahon CB. Fracture tolerance of the small female elbow joint in compression: the effect of load angle relative to the long axis of the forearm. *Stapp Car Crash J*. 2002;46:195-210.

[105] Duma SM, Boggess BM, Crandall JR, Hurwitz SR, Seki K, Aoki T. Upper extremity interaction with a deploying side airbag: a characterization of elbow joint loading. *Accid Anal Prev*. 2003;35(3):417-425.

[106] Duma SM, Crandall JR, Hurwitz SR, Pilkey WD. Small Female Upper Extremity Interaction with a Deploying Side Air Bag. Proceedings 42nd Stapp Car Crash Conference, Tempe, Arizona, November, 1998, Paper no.:983148.

[107] Duma SM, Crandall JR, Pilkey WD, Seki K, Aoki T. Dynamic Response of the Hybrid III 3 Year Old Dummy Head and Neck During Side Air Bag Loading. Proceedings of the Institution of Mechanical Engineers Part D - Journal of Automobile Engineering. 213(D5):471-480, 1999.

[108] Duma SM, Crandall JR, Pilkey WD, Seki K, Aoki T. Fifth percentile dummy upper extremity interaction with a deploying side air bag. Proceedings of the Institution of Mechanical Engineers Part D - Journal of Automobile Engineering. 217(D2):79-86, 2003.

[109] Duma SM, Crandall JR, Rudd RW, Kent RW. Small female head and neck interaction with a deploying side airbag. *Accid Anal Prev*. 2003;35(5):811-816.

[110] Duma SM, Crandall JR, Seki K, Aoki T. Comparison of the Q3 and Hybrid III 3 Year Old Dummy Head and Neck Response During Side Air Bag Loading. Proceedings of the Institution of Mechanical Engineers Part D - Journal of Automobile Engineering. 214(D7):675-684, 2000.

[111] Duma SM, Moorcraft DM, Gabler HC, Manoogian SM, Stitzel JD, Duma GG. Analysis of pregnant occupant exposure and the potential effectiveness of four-point seatbelts in far side crashes. Annu Proc Assoc Adv Automot Med. 2006;50:187-198.

[112] Duma SM, Hansen GA, Kennedy EA, Rath AL, McNally C, Kemper AR, Smith EP, Brolinson PG, Stitzel JD, Davis MB, Bass CR, Brozoski FT, McEntire BJ, Alem NM, Crowley JS. Upper extremity interaction with a helicopter side airbag: injury criteria for

dynamic hyperextension of the female elbow joint. *Stapp Car Crash J*. 2004;48:155-176.

[113] Duma SM, Kemper AR, Porta DJ. Biomechanical response of the human cervical spine. *Biomed Sci Instrum*. 2008;44:135-140.

[114] Duma SM, Kemper AR, McNeely DE, Brolinson PG, Matsuoka F. Biomechanical response of the lumbar spine in dynamic compression. *Biomed Sci Instrum*. 2006;42:476-481.

[115] Duma SM, Kemper AR, Stitzel JD, McNally C, Kennedy KA, Matsuoka F. Rib fracture timing in dynamic belt tests with human cadavers. *Clin Anat*. 2011;24(3):327-338.

[116] Duma SM, Manoogian SJ, Bussone WR, Brolinson PG, Goforth MW, Donnenwerth JJ, Greenwald RM, Chu JJ, Crisco JJ. Analysis of real-time head accelerations in collegiate football players. *Clin J Sport Med*. 2005;15(1):3-8.

[117] Duma SM, Moorcroft DM, Stitzel JD, Duma GG. Evaluating pregnant occupant restraints: the effect of local uterine compression on the risk of fetal injury. *Ann P Assoc Adv Automot Med*. 2004;48:103-114.

[118] Duma SM, Moorcroft DM, Stitzel JD, Duma GG. Biomechanical modeling of pregnant occupants in far-side vehicle crashes. *Biomed Sci Instrum*. 2006;42:154-159.

[119] Duma SM. Pregnant Occupant Biomechanics: Advances in Automobile Safety Research (2010) Published by the Society of Automotive Engineers, Warrendale PA.

[120] Duma SM, Rowson S. Past, present, and future of head injury research. *Exerc Sport Sci Rev*. 2011;39(1):2-3.

[121] Duma SM, Rudd RW, Crandall JR. A protocol system for testing biohazardous materials in an impact biomechanics research facility. *Am Ind Hyg Assoc J*. 1999;60(5):629-634.

[122] Duma SM, Schreiber P, McMaster JD, Crandall JR, Bass CR. Fracture Tolerance of the Male Forearm: the Effect of Pronation Versus Supination. Proceedings of the Institution of Mechanical Engineers Part D - Journal of Automobile Engineering. 216(D8):649-654, 2002.

[123] Duma SM, Schreiber PH, McMaster JD, Crandall JR, Bass CR, Pilkey WD. Dynamic injury tolerances for long bones of the female upper extremity. J Anat. 1999;194(Pt 3):463-471.

[124] Duma S, Stitzel J, Kemper A, McNally C, Kennedy E, Brolinson G, Matsuoka F. Acquiring non-censored rib fracture data during dynamic belt loading. *Biomed Sci Instrum*. 2006;42:148-153.

[125] Duma SM, Stitzel JD, Ryan LP, Crandall JR. Determination of Bone Mineral Content in Cadaveric Test Specimens. Journal of the Southern Orthopedic Association. 11(3):128-134, 2002.

[126] Funk JR, Rowson S, Daniel RW, Duma SM. Validation of concussion risk curves for collegiate football players derived from HITS Data. *Ann Biomed Eng*. 2012;40(1): 79-89.

[127] Funk JR, Duma SM, Manoogian SJ, Rowson S. Biomechanical risk estimates for mild traumatic brain injury. *Annu Proc Assoc Adv Automot Med*. 2007;51:343-361.

[128] Gayzik FS, Bostrom O, Ortenwall P, Duma SM, Stitzel JD. An experimental and computational study of blunt carotid artery injury. *Annu Proc Assoc Adv Automot Med*. 2006;50:13-32.

[129] Gayzik FS, Martin RS, Gabler HC, Hoth JJ, Duma SM, Meredith JW, Stitzel JD. Characterization of crash-induced thoracic loading resulting in pulmonary contusion. *J Trauma*. 2009;66(3):840-849.

[130] Gayzik FS, Tan JC, Duma SM, Stitzel JD. Mesh development for a finite element model of the carotid artery. *Biomed Sci Instrum*. 2006;42:187-192.

[131] Hurst WJ, Cormier JM, Stitzel JD, Jernigan MV, Moorcroft DM, Herring IP, Duma SM. A New Methodology for Investigating Airbag-induced Skin Abrasions, Proceedings of the Institution of Mechanical Engineers Part D - Journal of Automobile Engineering Vol. 219 (D5):599-605, 2005.

[132] Jernigan MV, Rath AL, Duma SM. Analysis of burn injuries in frontal automobile crashes. *J Burn Care Rehabil*. 2004;25(4):357-362.

[133] Jernigan MV, Duma SM. The effects of airbag deployment on severe upper extremity injuries in frontal automobile accidents. *Am J Emerg Med*. 2003;21(2):100-105.

[134] Jernigan MV, Rath AL, Duma SM. Severe upper extremity injuries in frontal automobile crashes: the effects of depowered airbags. *Am J Emerg Med*. 2005;23(2):99-105.

[135] Kemper AR, McNally C, Duma SM. Development of Stiffness Corridors for the Male and Female Arm. In: Proceedings of the 21st Enhanced Safety of Vehicles Conference, Stuttgart, Germany, 2009, Paper number: 09-0506.

[136] Kemper AR, Kennedy EA, McNally C, Manoogian SJ, Stitzel JD, Duma SM. Reducing chest injuries in automobile collisions: rib fracture timing and implications for thoracic injury criteria. *Ann Biomed Eng*. 2011;39(8):2141-2151.

[137] Kemper AR, McNally C, Pullins CA, Freeman LJ, Duma SM, Rouhana SM. The biomechanics of human ribs: material and structural properties from dynamic tension and bending tests. *Stapp Car Crash J*. 2007;51:235-273.

[138] Kemper AR, McNally C, Duma SM. Load Transfer and Deformation Characteristics of the Pelvis in Non-Destructive Side Impact Testing. In: Proceedings of the 21st Enhanced Safety of Vehicles Conference. Stuttgart, Germany, 2009, Paper number: 09-0508.

[139] Kemper AR, McNally C, Duma SM. The influence of strain rate on the compressive stiffness properties of human lumbar intervertebral discs. *Biomed Sci Instrum*. 2007;43:176-181.

[140] Kemper AR, McNally C, Duma SM. Acquiring non-censored pelvic bone fracture data during dynamic side impact loading – biomed 2009. Biomed Sci Instrum. 2009;45:395-400.

[141] Kemper AR, McNally C, Duma SM. Biofidelity of an original and modified SID-IIs upper extremity: matched cadaver and dummy compression tests. *Biomed Sci Instrum*. 2008;44:111-116.

[142] Kemper AR, McNally C, Duma SM. Dynamic compressive response of the human pelvis: axial loading of the sacroiliac joint. *Biomed Sci Instrum*. 2008;44:171-176.

[143] Kemper AR, McNally C, Duma SM. Dynamic tensile material properties of human pelvic cortical bone. *Biomed Sci Instrum*. 2008;44:417-418.

[144] Kemper AR, McNally C, Duma SM. The effect of the periosteum and straing on the structural response of human ribs – biomed 2009. *Biomed Sci Instrum*. 2009;45:12-17.

[145] Kemper AR, McNally C, Kennedy EA, Manoogian SJ, Duma SM. The influence of arm position on thoracic response in side impacts. *Stapp Car Crash J*. 2008;52:379-420.

[146] Kemper AR, McNally C, Kennedy EA, Manoogian SJ, Rath AL, Ng TP, Stitzel JD, Smith EP, Duma SM, Matsuoka F. Material properties of human rib cortical bone from dynamic tension coupon testing. *Stapp Car Crash J*. 2005;49:199-230.

[147] Kemper AR, McNally C, Manoogian SJ, Duma SM. Tensile material properties of human tibia cortical bone: effects of orientation and loading rate. *Biomed Sci Instrum*. 2008;44:419-427.

[148] Kemper AR, McNally C, Smith B, Duma SM. Quasi-linear viscoelastic characterization of human hip ligaments. *Biomed Sci Instrum*. 2007;43:324-329.

[149] Kemper AR, Ng TP, Duma SM. The biomechanical response of human bone: the influence of bone volume and mineral density. *Biomed Sci Instrum*. 2006;42:284-289.

[150] Kemper AR, Santago AC, Stitzel JD, Sparks JL, Duma SM. Biomechanical response of human spleen in tensile loading. *J Biomech*. 2012;45(2): 348-355.

[151] Kemper AR, Santago AC, Stitzel JD, Sparks JL, Duma SM. Biomechanical response of human liver in tensile loading. *Ann Adv Automot Med*. 2010;54:15-26.

[152] Kemper AR, Stitzel JD, McNally C, Gabler HC, Duma SM. Biomechanical response of the human clavicle: the effects of loading direction on bending properties. *J Appl Biomech*. 2009;25(2):165-174.

[153] Kennedy EA, Hurst WJ, Stitzel JD, Cormier JM, Hansen GA, Smith EP, Duma SM. Lateral and posterior dynamic bending of the mid-shaft femur: fracture risk curves for the adult population. *Stapp Car Crash J*. 2004;48:27-51.

[154] Kennedy EA, Tordonado DS, Duma SM. Effects of freezing on the mechanical properties of articular cartilage. *Biomed Sci Instrum*. 2007;43:342-347.

[155] Kent RW, Crandall JR, Bolton JR, Duma SM. Comparison and evaluation of contemporary restraint systems in the driver and front-passenger environments. Proceedings of the Institution of Mechanical Engineers Part D - Journal of Automobile Engineering. 215(D11):1147-1159, 2001.

[156] Kimpara H, Nakahira Y, Iwamoto M, Rowson S, Duma S. Head injury prediction methods based on 6 degree of freedom head acceleration measurements during impact. International Journal of Automotive Engineering. 2(2):13-19, 2011.

[157] Loftis K, Halsey M, Anthony E, Duma S, Stitzel J. Pregnant female anthropometry from CT scans for finite element model development. Biomed Sci Instrum. 2008;44:355-360.

[158] Manoogian SJ, Bisplinghoff JA, McNally C, Kemper AR, Santago AC, Duma SM. Effect of strain rate on the tensile material properties of human placenta. J Biomech Eng. 2009;131(9):091008.

[159] Manoogian SJ, Bisplinghoff JA, McNally C, Kemper AR, Santago AC, Duma SM. Dynamic tensile properties of human placenta. *J Biomech*. 2008;41(16):3436-3440.

[160] Manoogian SJ, Moorcroft DM, Duma SM. Pregnant occupant injury risk in severe frontal crashes using computer simulations. *Biomed Sci Instrum*. 2008;44:249-255.

[161] Manoogian S, Kennedy E, Wilson K, Duma S. Prevention of facial fractures from night vision goggle impact. *Biomed Sci Instrum*. 2006;42:13-18.

[162] Manoogian SJ, Kennedy EA, Wilson KA, Duma SM, Alem NM. Predicting neck injuries due to head-supported mass. *Aviat Space Environ Med*. 2006;77(5):509-514.

[163] Manoogian S, McNally C, Calloway B, Duma S. Methodology for dynamic biaxial tension testing of pregnant uterine tissue. *Biomed Sci Instrum*. 2007;43:230-235.

[164] Manoogian S, McNally C, Calloway B, Duma S, Mertz H. Utilizing cryogenic grips for dynamic tension testing of human placenta tissue. *Biomed Sci Instrum*. 2007;43:354-359.

[165] Manoogian SJ, McNally C, Stitzel JD, Duma SM. Dynamic biaxial tissue properties of pregnant porcine uterine tissue. *Stapp Car Crash J*. 2008;52:167-185.

[166] Manoogian S, McNeely D, Duma S, Brolinson G, Greenwald R. Head acceleration is less than 10 percent of helmet acceleration in football impacts. *Biomed Sci Instrum*. 2006;42:383-388.

[167] Manoogian SJ, Moorcroft DM, Duma SM. Evaluation of pregnant female injury risk during everyday activities. *Biomed Sci Instrum*. 2008;44:183-188.

[168] McGwin G Jr, Modjarrad K, Duma S, Rue LW 3rd. Association between upper extremity injuries and side airbag availabiliy. *J Trauma*. 2008;64(5):1297-1301.

[169] Moorcroft DM, Stitzel JD, Duma GG, Duma SM. Computational model of the pregnant occupant: predicting the risk of injury in automobile crashes. *Am J Obstet Gynecol*. 2003;189(2):540-544.

[170] Moorcroft DM, Stitzel JD, Duma S, Duma GG. The effects of uterine ligaments on the fetal injury risk in frontal automobile crashes. Proceedings of the Institution of

Mechanical Engineers Part D - Journal of Automobile Engineering. 217(D):1049-1055, 2003.

[171] Ng TP, Bussone WR, Duma SM. The effect of gender and body size on linear accelerations of the head observed during daily activities. *Biomed Sci Instrum*. 2006;42:25-30.

[172] Ng TP, Bussone WR, Duma SM, Kress TA. Thoracic and lumbar spine accelerations in everyday activities. *Biomed Sci Instrum*. 2006;42:410-415.

[173] Rath AL, Jernigan MV, Stitzel JD, Duma SM. The effects of depowered airbags on skin injuries in frontal automobile crashes. *Plast Reconstr Surg*. 2005;115(2):428-435.

[174] Rowson S, Duma SM, Beckwith JG, Chu JJ, Greenwald RM, Crisco JJ, Brolinson PG, Duhaime AC, McAllister TW, Maerlender AC. Rotational dead kinematics in football impacts: an injury risk function for concussion. *Ann Biomed Eng*. 2012;40(1):1-13.

[175] Rowson S, Beckwith JG, Chu JJ, Leonard DS, Greenwald RM, Duma SM. A six degree of freedom head acceleration measurement device for use in football. *J Appl Biomech*. 2011;27(1):8-14.

[176] Rowson S, Brolinson G, Goforth M, Dietter D, Duma S. Linear and angular head acceleration measurements in collegiate football. *J Biomech Eng*. 2009;131(6):061016.

[177] Rowson S, Duma SM. Development of the STAR evaluation system for football helmets: integrating player head impact exposure and risk of concussion. *Ann Biomed Eng*. 2011;39(8):2130-2140.

[178] Rowson S, Goforth MW, Dietter D, Brolinson PG, Duma SM. Correlating cumulative sub-concussive impacts in football with player performance. *Biomed Sci Instrum*. 2009;45:113-118.

[179] Rowson S, McNally C, Duma SM. In situ measurement of Achilles tendon tension during dorsiflexion – biomed 2009. *Biomed Sci Instrum*. 2009;45:18-23.

[180] Rowson S, McNally C, Duma SM. Can footwear affect Achilles tendon loading? Clin J Sport Med. 2010;20(5):344-349.

[181] Rowson S, McNeely DE, Duma SM. Differences in Hybrid III and THOR-NT neck response in extension using matched tests with football neck collars. *Biomed Sci Instrum*. 2008;44:165-170.

[182] Rowson S, McNeely DE, Duma SM. Force transmission to the mandible by chin straps during head impacts in football. *Biomed Sci Instrum*. 2008;44:195-200.

[183] Rowson S, McNeely DE, Duma SM. Lateral bending biomechanical analysis of neck protection devices used in football. *Biomed Sci Instrum*. 2007;43:200-205.

[184] Rowson S, McNeely DE, Brolinson PG, Duma SM. Biomechanical analysis of football neck collars. *Clin J Sport Med*. 2008;18(4):316-321.

[185] Santago AC, Kemper AR, McNally C, Sparks JL, Duma SM. Freezing affects the mechanical properties of bovine liver – biomed 2009. *Biomed Sci Instrum*. 2009;45:24-29.

[186] Santago AC, Cormier JM, Duma SM. Humerus fracture bending risk function for the 50th percentile male. *Biomed Sci Instrum*. 2008;44:231-236.

[187] Santago AC, Cormier JM, Duma SM, Yoganandan N, Pintar FA. Forearm fracture bending risk function for the 50th percentile male. *Biomed Sci Instrum*. 2008;44:201-206.

[188] Santago AC, Kemper AR, McNally C, Sparks JL, Duma SM. The effect of temperature on the mechanical properties of bovine liver – biomed 2009. *Biomed Sci Instrum*. 2009;45:376-381.

[189] Shain KS, Madigan ML, Rowson S, Bisplinghoff J, Duma SM. Analysis of the ability of catcher's masks to attenuate head accelerations on impact with a baseball. *Clin J Sport Med. 2010;*20(6):422-427.

[190] Stitzel J, Kemper A, Duma S. Myopia and hyperopia's effect on probability of globe rupture due to a foreign body impact. *Invest Ophthalmol Vis Sci.* 2005;46.

[191] Stitzel JD, Barretta JT, Duma SM. Predicting fractures due to blunt impact: a sensitivity analysis of the effects of altering failure strain of human rib cortical bone. International Journal of Crashworthiness. 9(6):633-642, 2004.

[192] Stitzel JD, Cormier JM, Barretta JT, Kennedy EA, Smith EP, Rath AL, Duma SM, Matsuoka F. Defining regional variation in the material properties of human rib cortical bone and its effect on fracture prediction. *Stapp Car Crash J.* 2003;47:243-265.

[193] Danelson KA, Gayzik FS, Yu MM, Martin RS, Duma SM, Stitzel JD. Bilateral carotid artery injury response in side impact using a vessel model integrated with a human body model. *Ann Adv Automot Med.* 2009;53:271-279.

[194] Stitzel JD, Gayzik FS, Hoth JJ, Mercier J, Gage HD, Morton KA, Duma SM, Payne RM. Development of a finite element-based injury metric for pulmonary contusion part I: model development and validation. *Stapp Car Crash J*. 2005;49:271-289.

[195] Takhounts EG, Ridella SA, Hasija V, Tannous RE, Campbell JQ, Malone D, Danelson K, Stitzel J, Rowson S, Duma S. Investigation of traumatic brain injuries using the next generation of simulated injury monitor (SIMon) finite element head model. *Stapp Car Crash J*. 2008;52:1-31.

[196] Weaver AA, Kennedy EA, Duma SM, Stitzel JD. Evaluation of different projectiles in matched experimental eye impact simulations. *J Biomech Eng*. 2011;133(3):031002.

[197] Yu MM, Manoogian SJ, Duma SM, Stitzel JD. Finite element modeling of human placental tissue. *Ann Adv Automot Med*. 2009;53:257-270.